Biomedicine & Pharmacotherapy 149 (2022) 112842

Contents lists available at ScienceDirect

Biomedicine & Pharmacotherapy

journal homepage: www.elsevier.com/locate/biopha

Chemical profiles and pharmacological insights of *Anisomeles indica* Kuntze: An experimental chemico-biological interaction

Suaad Nasrin [a], Mohammad Nazmul Islam [a], Mohammed Abu Tayab [a], Mst. Samima Nasrin [a,b], Md. Abu Bakar Siddique [c], Talha Bin Emran [d,e,*], A.S.M. Ali Reza [a,b,**]

[a] Department of Pharmacy, International Islamic University Chittagong, Chittagong 4318, Bangladesh
[b] Department of Biochemistry and Molecular Biology, University of Chittagong, Chittagong 4331, Bangladesh
[c] Institute of National Analytical Research and Service (INARS), Bangladesh Council of Scientific and Industrial Research (BCSIR), Dhaka 1205, Bangladesh
[d] Department of Pharmacy, BGC Trust University Bangladesh, Chittagong 4381, Bangladesh
[e] Department of Pharmacy, Faculty of Allied Health Sciences, Daffodil International University, Dhaka 1207, Bangladesh

ARTICLE INFO

Keywords:
Anisomeles indica
MeOH-AI
Anti-inflammatory
Thrombolytic
Anti-depression
Antidiarrheal

ABSTRACT

Anisomeles indica (L.) Kuntze is an ethnomedicinally important plant that has long been used in traditional medicine to treat a variety of ailments, including dyspepsia, abdominal pain, colic, allergies, inflammation, and rheumatic arthritis. However, the scientific framework underlying these medicinal properties is not well known. This study aimed to investigate the antidepressive, antidiarrheal, thrombolytic, and anti-inflammatory potential of a methanol extract of *A. indica* (MeOH-AI). The potential bioactive compounds in the MeOH-AI were identified using gas chromatography-mass spectrometry (GC-MS), and antidepressant activities were evaluated using the tail suspension test (TST) and forced swim test (FST). Antidiarrheal effects were also assayed in castor oil-induced diarrhea and gastrointestinal motility studies. The anti-inflammatory activities were explored by examining the effects on protein inhibition and denaturation in heat- and hypotonic solution-induced hemolysis assays. The thrombolytic activity was evaluated using the clot lysis test in human blood. BIOVIA and Schrödinger Maestro (v11.1) were applied for docking analysis to determine binding interactions, and the absorption, distribution, metabolisms, excretion/toxicity (ADME/T) properties of bioactive compounds were explored using a web-based method. The GC-MS analysis of MeOH-AI revealed the presence of several bioactive compounds. MeOH-AI administration resulted in significant ($p < 0.01$) reductions in the immobility times for both the FST and TST compared with those in the control group. MeOH-AI also induced significant ($p < 0.01$) reductions in castor oil-induced diarrhea severity and gastrointestinal motility in a mouse model. In addition, the *in vitro* anti-inflammatory and thrombolytic activity studies produced remarkable responses. The binding assay showed that 4-dehydroxy-N-(4,5-methylenedioxy-2-nitrobenzylidene) tyramine interacts favorably with monoamine oxidase and serotonin and M3 muscarinic acetylcholine receptors, displaying good pharmacokinetic properties, which may mediate the effects of MeOH-AI on depression and diarrhea. Overall, the research findings indicated that MeOH-AI has significant antidepressant, antidiarrheal, and anti-inflammatory effects and may represent an alternative source of novel therapeutic factors.

1. Introduction

Many medicinal plants can be found in the rural and hill tract areas of Bangladesh. Herbs and natural products are highly valuable sources of bioactive compounds, and their benefits and usefulness for the treatment of various diseases have long been recognized [1–4]. Plants and

Abbreviations: ADME/T, absorption, distribution, metabolism, excretion, and toxicity; ANOVA, one-way analysis of variance; BSA, Bovine serum albumin; COX, Cyclooxygenase; p.o., per oral; i.p., Intraperitoneal; BOD, biochemical oxygen demand; FCR, Folin-Ciocalteu reagent; GAE, Gallic acid equivalent; HRBC, Human red blood cell; ROS, Reactive oxygen species; NC, Vehicle or Negative control; NSAID, Non-steroidal anti-inflammatory drug; PBS, Phosphate-buffered saline; QE, Quercetin; RC, Reference or positive control; SEM, Standard error mean; TNF-alpha, tumor necrosis factor-alpha.

* Correspondence to: Department of Pharmacy, BGC Trust University Bangladesh, Chittagong, Chandanaish, 4381, Bangladesh.
** Corresponding author at: Department of Pharmacy, International Islamic University Chittagong, Chittagong 4318, Bangladesh.
E-mail addresses: talhabmb@bgctub.ac.bd (T.B. Emran), alirezaru@gmail.com (A.S.M.A. Reza).

https://doi.org/10.1016/j.biopha.2022.112842
Received 18 December 2021; Received in revised form 14 March 2022; Accepted 16 March 2022
Available online 21 March 2022

their secondary metabolites are key factors in the discovery and development of novel therapeutic agents [5–7]. The search for new drugs derived from plants has become increasingly focused during the last couple of decades. *Anisomeles indica* (L.) Kuntze belongs to the Lamiaceae family. Commonly known as gobura (catmint), *A. indica* is an annual aromatic shrub that can be found throughout Bangladesh. The *A. indica* has been used for the treatment of diverse conditions such as inflammatory skin diseases, liver disease and protection, gastrointestinal disease and hypertension, and immune system deficiencies [8]. The leaves of *A. indica* are frequently used to treat whooping cough and fever in infants [9,10]. For centuries, the roots of *A. indica* have been used to treat allergies, uterine infections, sores, and mouth abscesses [11], and the roots have also been described as displaying anti-inflammatory, astringent, and tonic properties [10]. The decoction of the leaves and roots of *A. indica* is used as traditional medicine for the management of colic, dyspepsia, hypertension, abdominal pain, and fever [10,12]. Moreover, the decoction of the shrub is used to treat epileptic convulsions [13]. The essential oil distilled from the leaves is applied externally as an embrocation in rheumatic arthritis [12]. In addition, the extracts of *A. indica* demonstrated that a decoction from the pre-flowering stage leaves and stems has anti-histaminergic, free radical scavenging, membrane stabilizing, and cyclooxygenase-I inhibitory activities [14]. Aqueous and alcoholic extracts derived from *A. indica* are effective against inflammatory mediators, microbes, cell proliferation, and melanogenesis [15–18]. Another study aqueous *A. indica* extract indicated analgesic effects [19]. Wang and Huang reported that the ethanol extract of *A. indica* exhibited strong anti-*Helicobacter pylori* activity [20]. In the Ellman method, the ethyl-acetate extracts of *A. indica* showed significant inhibitory activity against both the acetylcholinesterase (IC_{50} = 176.02 ± 7.31 μg/mL) and butyrylcholinesterase enzymes (IC_{50} = 143.83 ± 6.04 μg/mL) [21]. The areal part of this plant possesses significant antiepileptic activity against in the pentylenetetrazole-induced convulsions model [13]. Previously, our research group showed that the methanol extract of *A. indica* (MeOH-AI) displayed anti-nociceptive, anxiolytic, and sedative activities in animal and computer-aided models [11]. The promising activities of MeOH-AI identified by our previous evaluation led to the design of the current research, which includes a more detailed profile of the bioactive compounds in MeOH-AI, as determined by gas chromatograph-mass spectrometry (GC-MS) analysis, and the evaluation of potential pharmacological (antidepressant, antidiarrheal, anti-inflammatory, and thrombolytic) activities. To characterize potential novel compounds and explore their possible mechanisms of action, we used *in silico* molecular docking and absorption, distribution, metabolism, excretion/toxicity (ADME/T) analyses.

The development of psychiatric disorders is influenced by a variety of genetic, social, psychological, and biological factors [22]. Consequently, chronic pain and inflammation are often associated with the onset of depression and anxiety [23,24]. Depression is the second most common mental illness, afflicting 21% of the global population. The activation of certain 5-hydroxytryptamine (5-HT, also known as serotonin) receptors, such as 5-HT_6, may be involved in mediating depression [25]. Currently, monoamine oxidase A (MAO-A) inhibitors are used for the treatment of depressive disorders to prevent the MAO-induced catalysis of 5-HT [26,27]. Bupropion is an efficient antidepressant with fewer side effects compared with other antidepressants due to its ability to inhibit norepinephrine and dopamine reuptake [28]. MAOIs and tricyclic antidepressants (TCAs) are common therapeutic agents used to prevent the upregulation of monoamine metabolism and block reuptake capacity [29]; however, many of the known therapeutic options for depression treatment are associated with unfavorable side effects [30]. New antidepressant medications are, therefore, being explored to avoid these drawbacks. Inflammation is a condition characterized by a localized surge in the number of leukocytes and the production of various complex mediators [31], typically characterized by recurring symptoms, such as redness, swelling, heat, and pain, and can lead to exudation and loss of function [32]. Various mediators and potent chemical compounds found in body tissues are known to be involved in inflammatory processes, such as prostaglandins, leukotrienes, prostacyclin, lymphocytes, and chemokines, including interferon (IFN)-α and -γ, interleukin (IL)− 1, IL-8, histamine, 5-HT, and tumor necrosis factor (TNF)-α [4,33,34]. Macrophages also play an important role in the immune response by regulating inflammatory responses and tissue remodeling, recovery, and healing processes [35,36]. The development of clots, also known as thrombus, within the circulatory system due to dysfunctional hemostasis can lead to vascular blockage and complications, such as those observed in atherothrombotic diseases [34,37].

Diarrhea is characterized by the movement of abnormal liquids or unformed stools through the digestive system, associated with elevated defecation frequency and abdominal pain [38,39]. Every year, 2.5 million children die worldwide from diarrhea-associated complications, and 80% of these deaths occur in developing countries [40]. The most popular treatment for diarrhea is oral rehydration using saline. In its guidelines for diarrheal management, the World Health Organization has acknowledged the accepted use of traditional medical practices. Natural antidiarrheal agents include kaolin, pectin, berberine, and muscarinic agents, in addition to morphine, codeine, and paregoric [41,42]. Based on our previous findings and the need for new therapeutic agents, the current study was designed to evaluate the anti-inflammatory, antidepressant, and antidiarrheal activity of MeOH-AI in a mouse model.

2. Materials and methods

2.1. Plant sample

The whole-plant sample of *A. indica* (L.) Kuntze was obtained from the Rajshahi University premises in Bangladesh in September 2012, which was authenticated by an expert taxonomist, Dr. Sheikh Bokhtear Uddin, at the University of Chittagong, Department of Botany. A voucher specimen has been conserved at the institutional herbarium at the University of Chittagong, Department of Botany (accession no. 1304).

2.2. Identification of bioactive compounds by gas chromatography

2.2.1. Extract preparation

A. indica (whole-plant) was shade-dried and powdered, and 500 g of the powder was placed in an amber bottle for extraction with absolute methanol (1500 mL). A 7-day thorough extraction was performed with intermittent stirring, rotating every 3 days. The combined extracts were filtered and concentrated under reduced pressure using a rotary evaporator, which produced approximately 16 g of a black-green semisolid, referred to as the MeOH-AI. This extract was utilized in the gas chromatographic analysis.

2.2.2. Sample analysis

In order to detect the bioactive components, present in *A. indica,* the whole-plant extract, MeOH-AI was examined by an electron impact ionization process in a mass spectrometer (MS, TQ 8040, Shimadzu Corporation, Kyoto, Japan) and a gas chromatograph (GC-17A, Shimadzu Corporation), fused to a silica capillary (Rxi-5 ms, 0.25 m, 30 m long, internal diameter: 0.32 mm) covered with DB-1 (J & W). The oven temperature was programmed at a starting temperature of 70 ℃ (0 min) increasing to 150 ℃, at 10 ℃/sec, with a hold time of 10 min, and the inlet temperature was maintained at 260 ℃. A rate of 0.6 mL/min was used for the flux at a constant pressure of 90 kPa using helium gas. The temperature interface between the GC and MS was maintained at a constant temperature of 280 ℃. The MS was performed using scan mode, with a range from 40 to 350 amu. The sample injection volume was 1 μL, and the entire GC-MS process lasted for 50 min [43]. A comparison with the GC-MS library (version 08-S) of the National

Institute of Standards and Technology (NIST) was performed to identify the compounds in peak areas. The sample was analyzed at the Institute of National Analytical Research and Service (INARS, ISO/IEC 17025:2017 accredited laboratory), Bangladesh Council of Scientific and Industrial Research (BCSIR), Dhaka, Bangladesh.

2.3. Analysis of chemical elements by spectrophotometric techniques

2.3.1. Chemicals and standards

Analytical grade nitric acid and perchloric acid were purchased from Fluka Analytical, Sigma-Aldrich, Germany. NIST (National Institute of Standards and Technology, USA) traceable Certified Reference Materials (CRM) for all chemical elements was also purchased from Fluka Analytical, Sigma-Aldrich, Germany. Analytical grade drugs and chemicals were used in this experiment and were obtained from MERCK, India; Sigma-Aldrich, USA; and Popular Pharmaceuticals Ltd. Bangladesh. All chemicals and standards were used as received without further purifications. Deionized (DI) water (electrical conductivity: 0.2 μS cm^{-1}, resistivity: 18.2 MΩ cm at 25 °C) was used for all samples and standard preparations.

2.3.2. Sample preparation

The fresh *A. indica* whole-plant were washed carefully with tap water and then with DI water and naturally air-dried [11]. The whole-plant were then cut into small pieces, and a definite weight of the whole-plant was taken in three previously cleaned and weighed glass beakers (250 mL) at the same time using a digital electrical balance (Model: GR-200, A&D Company Ltd., Tokyo, Japan). The whole-plants in the beakers were then dried in an electrical oven at 110 ℃ for 24 h, and the weight loss was recorded after cooling the beaker in a desiccator for the estimation of moisture content. The beakers containing the oven-dried whole-plant were then placed in an electrical Muffle furnace and heated gradually to 600 ℃, using a controlled temperature-program, which increases the temperature at 50 ℃ intervals, maintaining the whole-plant at each temperature interval at least for 30 ℃. After rising the temperature to 600 ℃, the heating continued for 6 h. The samples were then cooled to room temperature, and the weight loss was recorded again for the determination of the amount of ash as well as organic matter upon burning the plant organic material. The samples in the beakers were then treated with concentrated nitric acid and perchloric acid (at a 2:1 ratio) and boiled on a hot plate at 150–180 ℃ until a colorless solution was obtained. The solutions were cooled and transferred to the calibrated volumetric flasks (100 mL), and the beakers were rinsed with DI water 3–5 times. The flasks were made up to the mark with DI water and then shaken well for homogeneity. The solutions were filtered and preserved in non-transparent plastic bottles at 4 ℃ for elemental analysis. A sample blank (adding no sample) was also prepared for quality control following the same procedure described above.

2.3.3. Sample analysis and analytical quality control

The sample was analyzed at the ISO/IEC 17025:2017 accredited laboratory of BCSIR (INARS), Dhaka, Bangladesh for 11 chemical elements including Cd, Mn, Co, Ni, Cu, Fe, Zn, Ca, Mg, K, and P. The concentrations of all chemical elements (except P) were estimated using atomic absorption spectrophotometer (AAS, Model: AA240FS, Varian, Australia). The elements Cd, Mn, Co, Ni, Cu, Fe, Zn, Mg, and K were analyzed in an air/acetylene flame, whereas Ca were analyzed in an air/nitrous oxide/acetylene flame, using atomic absorption technique. K was determined using the atomic emission technique in AAS. The concentration of P in the sample was determined using an ultraviolet-visible spectrophotometer (Model: UV-1650PC, Shimadzu, Japan). The physical parameters such as moisture, ash, and organic matter content were estimated by measuring the weight differences of the sample after drying and ashing. All physical and chemical parameters were analyzed separately in each of the three replicate samples (see Section 2.3.2), and their average values were reported. An individual CRM for each element was used to prepare working standard solutions for the construction of the calibration curve (linearity: ≥ 0.99) for each chemical element. The accuracy and precision of the analysis were verified by the simultaneous analysis of a known concentration of CRM and the replicate analysis of the same samples, respectively (relative standard deviation, RSD, for all measurements was less than 5%). The spike recovery values (%) for all analyses were within 90%− 110% and were calculated using equations reported elsewhere [44,45]. Further details regarding the analytical procedures and the quality control measures were reported earlier [46].

2.4. Animals

Six to seven-week-old Swiss albino mice of both sexes, weighing 25–40 g, were obtained from the International Centre for Diarrheal Disease and Research (ICDDR), Dhaka, Bangladesh. Animals were housed in polycarbonate cages and maintained in a standard laboratory environment of 25 ℃ temperature and 55–60% humidity in a 12-hours daylight cycle. Mice had free access to an animal pellet diet and tap water. The Planning and Development (P & D) Committee of the Department of Pharmacy, International Islamic University Chittagong, Bangladesh, approved the animal handling procedures (Pharm-P&D-138/13-'19).

2.5. Acute oral toxicity test

The acute oral toxicity test of MeOH-AI was carried out following the previously described protocol [47], with minor modifications. MeOH-AI was administered orally at doses of 500, 1000, 2000, and 4000 mg/kg body weight (b.w.) to groups of six Swiss albino mice each, which were fasted for 18 h before the dose administration. Individual mice were kept under careful observation for the first 30 min after dosing, then every 24 h (with special attention paid to the first 3–4 h) for the next 72 h to monitor delayed toxicity such as itching, skin rash, swelling, autonomic and CNS changes. Based on the outcomes of this toxicity test and the possible median lethal dose, the effective dose was chosen for evaluating the *in vivo* pharmacological effects of MeOH-AI.

2.6. Antidepressant bioassay

2.6.1. Experimental design

For each *in vivo* antidepressant model, a total of 24 Swiss albino mice (12 males and 12 females) were randomly divided into four groups (n = 6). The treatment protocol was designed as follows: the negative control (NC) group received 1% Tween 80 in water at 10 mL/kg b.w., the positive or reference control (RC) group received imipramine HCl at 10 mg/kg b.w., and the two test groups received MeOH-AI at doses of 200 and 400 mg/kg b.w. All regimens were delivered orally via gavage.

2.6.2. Tail suspension test

The tail suspension test (TST) was performed as described in a previous protocol [48] to test the antidepressant effects of MeOH-AI in a mouse model. As indicated in 2.6.1., each experimental animal group was treated with either vehicle, reference standard, or test sample. Two stands, each with a clamp located 22 cm from the floor, were placed at intervals of 23 cm. A mouse was hung 5 cm (to inflict depression) from the end of its tail on a stand and observed for 6 min. The average immobility period for each group was recorded during the last 4 min from the total observation of 6 min. Inhibition percentage was calculated as follows:

$$\text{Inhibition } (\%) = (A - B) / A \times 100$$

where A = immobile time in the control group and B = immobile time in the test group.

2.6.3. Forced swim test

The forced swim test (FST) was performed to examine the antidepressant activity of MeOH-AI using a previously described protocol and mouse model [49]. Thirty minutes after the treatment (as described in Section 2.6.1.), each mouse was individually placed in an open glass compartment (diameter: 10 cm, height: 25 cm) filled with freshwater (25 ± 1 °C) to a height of 19 cm. The mice were then tracked for 6 min. The first 2 min were referred to as the initial setting time, and the following 4 min were reported as the time of immobility. The mouse was considered to be still when it was floating without motion or was only treading water to keep its nose above the water surface. After the observation, the mice were carefully removed from the water and then properly dried before being returned to their home cages. The percentage of immobility inhibition was calculated as follows:

$$\text{Inhibition } (\%) = (A - B) / A \times 100$$

where A = immobile time in the control group and B = immobile time in the test group.

2.7. Antidiarrheal bioassay

2.7.1. Castor oil-triggered diarrhea

The antidiarrheal effects of MeOH-AI were examined using the Taufiq and Bellah process [50,51]. Swiss Albino mice were fasted for 24 h and separated into four groups (n = 6). The first group (i.e., NC group) was treated orally with a normal dose of 10 mL/kg b.w. of Tween 80 (1% Tween 80 in water); the second group received (i.e., RC group) orally loperamide at 5 mg/kg b.w., and the test groups were treated orally with 200 and 400 mg/kg b.w. of MeOH-AI. One hour after treatment administration, castor oil was administered (0.5 mL). Mice were housed in separate cages lined with transparent paper, modified hour by hour to increase fecal visibility. Droppings were counted for 4 h at intervals of 60 min. The NC and RC groups have compared the average number of stools passed to treated groups. The average amount of diarrhea, assessed as the pooled quantity among all mice in the control group, was set to 100%. The inhibition (%) of defecation following treatment was determined with the following equation relative to control the control value:

$$\text{Inhibition of defecation } (\%) = [(\text{NDC} - \text{NDT}) / \text{NDC}] \times 100$$

where NDC = mean number of diarrheic droppings in the control group and NDT = mean number of diarrheic droppings in the treated group.

2.7.2. Gastrointestinal motility

The gastrointestinal (GI) motility assessment was performed using the technique described by Mascolo [52]. Swiss albino mice were fasted for 24 h with free access to water and divided into 4 groups ($n = 6$). The first group received 10 mL/kg b.w. of Tween 80 (1% Tween 80 in water) as the NC group, the second group received 5 mg/kg b.w. of loperamide as the RC group, and the two test groups received 200 and 400 mg/kg b.w. of MeOH-AI. One hour later oral administration of treatments, animals were fed 1 mL of a charcoal meal (10% charcoal suspension in 5% gum acacia) orally. After 1 h, the animals were sacrificed using 70% (v/v) ethanol in 0.9% sterile saline as an anesthetic, and the distance traveled by the charcoal meal from the pylorus to the caecum was measured and expressed as a percentage of the total distance of the intestine. The percentage inhibition was calculated using the following formula:

$$\text{Inhibition}(\%) = \frac{\text{Distance travelled by the } \textit{control} - \text{Distance travelled by the } \textit{test}}{\text{Distance travelled by the } \textit{control}} \times 100$$

2.8. In vitro anti-inflammatory activity

2.8.1. Inhibition of protein denaturation

The anti-inflammatory effects of MeOH-AI were explored using a protein denaturation technique, with minor changes [53]. The reaction mixture (0.5 mL) was comprised of bovine serum albumin (BSA, 0.45 mL) and MeOH-AI (0.05 mL), and various concentrations of standard solution were generated (31.25, 62.5, 125, 250, and 500 μg/mL) using diclofenac sodium as the standard. The sample was heated at 37 ℃ for 20 min and held at 57 ℃ for another 30 min. Furthermore, the previous solutions had a 2.5 mL phosphate buffer, and absorption (Abs) was measured at 660 mm using a spectrophotometer; a negative control contained only distilled water. Triplicate tests were performed, and the inhibition protein denaturation was determined as follows:

$$\text{Inhibition}(\%) = \frac{\text{Abs}^{\text{control}} - \text{Abs}^{\text{test}}}{\text{Abs}^{\text{control}}} \times 100$$

2.8.2. Heat-induced hemolysis

Aliquots (5 mL) of an isotonic buffer containing 1 mg/mL of the extract were separated into two duplicate sets of centrifuge tubes [39]. A similar volume of vehicle and an erythrocyte suspension (30 μL) was added to each tube, which was mixed by mild inversion. One tube was incubated in a water bath at 54 ℃ for 20 min, whereas the other was incubated in an ice bath at 0–5 ℃. The mixtures were centrifuged for 3 min, and the absorbance of the supernatant was measured at 540 nm. The percentage of hemolysis inhibition tests was determined based on the following equation:

$$\text{Hemolysis inhibition } (\%) = 100 \times [1 - (\text{OD2} - \text{OD1} / \text{OD3} - \text{OD1})]$$

2.8.3. Hypotonic solution-induce hemolysis

The methods used were based on standard techniques for an *in vitro* membrane stability assay [54]. Briefly, a 0.5 mL of human red blood cell (HRBC) suspension was mixed with 1 mL phosphate buffer (pH 7.4) and 2 mL hypotonic-saline, followed by the addition of the plant extract (0.5 mL) or the standard drug acetyl salicylic acid (500, 250, and 125 μg/mL). The extracts were incubated for 30 min at 37 ℃, followed by centrifugation for 10 min, and the absorbance of the supernatant was measured at 540 nm. Hemolysis inhibition was calculated as follows:

$$\text{Hemolysis inhibition } (\%) = 100 \times [(\text{OD1} - \text{OD2}) / \text{OD1}]$$

where, OD1 = optical density of hypotonic-buffered saline solution alone (control) and OD2 = optical density of test sample in hypotonic solution.

2.9. In vitro thrombolytic activity

MeOH-AI was tested for clot lysis abilities using the procedure described by Prasad et al. [55]. A 7 mL volume of venous blood was retrieved from healthy volunteers (n = 7) who had no history of smoking, alcoholism, consuming lipid-lowering medications, oral contraceptive use, or anticoagulant treatment. Blood samples were transferred to sterile, pre-weighted micro-centrifuge tubes (1 mL/tube), followed by incubation for 45 min at 37 ℃. After a clot formed, the serum was fully

extracted from the tubes (without disrupting the clot), and each tube containing a clot was measured again to determine the clot's weight. A 100 μL solution of MeOH-AI at a concentration of 10 mg/mL was added separately to each microcentrifuge tube containing a pre-weighed clot. Then, 100 μL of distilled water and 100 μL of streptokinase were transferred to separate microcentrifuge tubes as positive control and negative control, respectively. After that, all of the tubes were incubated at 37 °C for 90 min to check for clot lysis. The obtained fluid was extracted from each tube after incubation, and the tubes were measured again to identify any difference in weight after the clot was disrupted. Finally, the weight difference was determined, and the result was expressed as a percentage of clot lysis, using the equation below:

Clot lysis (%) = (weight of the clot after lysis) / (weight of clot before lysis) × 100

2.10. In silico study

2.10.1. Chemical compounds studied

The following 12 identified compounds in MeOH-AI were examined: α.-humulene (PubChem CID: 5281520); 2,6,10,14,18,22-tetracosahexaene, 2,6,10,15,19,23-hexamethyl-, (all-E)- (PubChem CID: 638072); 4-dehydroxy-N-(4,5-methylenedioxy-2-nitrobenzylidene)tyramine (PubChem CID:610062); stigmasterol (PubChem CID:5280794); neophytadiene(PubChem CID: 10446); 2-hexadecen-1-ol, 3,7,11,15-tetramethyl-, [R-[R* ,R* -(E)]]- (PubChem CID: 5366244); bicyclo[8.1.0] undecane (PubChem CID:527597); 2-(4-methylphenyl)ethynylaniline (PubChem CID:14341826); vitamin E (PubChem CID:14985); ethane, 1-(4,4,4-trifluoro-1,3-dithiobutyl)− 2-(3,3,3-trifluoro-1,2-dithiopropyl)- (PubChem CID: 610064); hexadecanoic acid, methyl ester (PubChem CID:8181); and cis-13-octadecenoic acid, methyl ester (PubChem CID: 12541027).

2.10.2. Molecular docking

Based on the GC-MS analysis, 12 major bioactive compounds identified in MeOH-AI were selected for the performance of molecular docking studies to gain insights into their potential molecular interactions with key therapeutic target proteins associated with inflammation, thrombosis, depression, and diarrhea. Docking experiments were conducted using the Schrödinger Suite-Maestro v11.8 (Schrödinger LLC, New York, NY, USA, 2018), and protein-ligand interactions were visualized using BIOVIA Discovery Studio Visualizer v21.1.0.20298 (BIOVIA, San Diego, CA, USA).

2.10.3. Ligand preparation

The two-dimensional (2D) chemical structures of the selected major compounds identified in MeOH-AI and the reference standard drugs, including diclofenac, streptokinase, fluoxetine, phenelzine, loperamide, and alosetron (PubChem CID 3033, 9815560, 3386, 3675, 3955, and 2099, respectively) were retrieved from the PubChem database (https://pubchem.ncbi.nlm.nih.gov). The structures were introduced into Schrödinger's Maestro v11.8, and the LigPrep tool was applied to prepare the ligands by neutralization at pH 7.0 ± 2.0 via Epik (version 4.6) [56], followed by minimization using the OPLS3e force field.

2.10.4. Receptor preparation

The complex crystal structures of target proteins associated with inflammation, thrombosis, depression, and diarrhea, including cyclooxygenase 2 (COX-2), tissue plasminogen activator (TPA), serotonin transporter 3 (SERT3), monoamine oxidase A (MAO-A), M3 muscarinic acetylcholine receptor (M3MACR), and 5-HT3 receptor were retrieved from Protein Data Bank (PDB) database (http://www.rcsb.org) using the PDB codes 4PH9 [57], 1A5H [58], 5I6X [59], 2Z5Y [60], 4U14 [61], and 5AIN [62], respectively. The proteins were refined, optimized, and minimized for docking experiments using the Protein Preparation Wizard integrated into the Schrödinger Suite-Maestro v11.8, according to methods reported earlier [63].

2.10.5. Grid generation and molecular docking

Glide (version 8.1), contained in Schrödinger Maestro v11.8, was used to create the receptor grid and conduct docking analysis [64,65]. For each processed protein, a grid was formed, retaining all parameters at the default settings, as described previously [63]. Subsequently, flexible ligand docking was executed using the Glide-Standard Precision scoring function under default parameters without receptor-ligand constraints. Compounds demonstrating optimally favorable binding energies against the examined proteins were ranked according to the maximum negative docking value.

2.11. Statistical analysis

All data are reported as the mean ± the standard error of the mean (SEM). One-way analysis of variance (ANOVA) was applied to assess differences among groups, followed by Dunnett's post hoc test, using GraphPad Prism software, version 6. P-values < 0.05 and < 0.01 were considered significant.

3. Results

3.1. GC-MS analysis

A total of 46 compounds were identified from the whole plant of *A. indica* using GC-MS, and their chemical compositions are indicated in Fig. 1 and Table 1. The total ionic chromatogram (TIC) is shown in Fig. 1. Twelve compounds were selected for molecular docking analyses because the specific biological activities of interest have not yet been established for these compounds.

3.2. Chemical elements and some physical parameters

Results of some chemical elements and physical parameters for *A. indica* are shown in Table 2. The concentration of the analyzed chemical elements revealed that *A. indica* contains a significant amount of essential chemical elements, indicating its good nutritive values. Further, the studied plant species showed a large percentage (96.97%) of organic matter upon burning at 600 ℃ in the Muffle furnace under air, which is an indication of the presence of a considerable amount of organic compounds in *A. indica*.

3.3. Acute oral toxicity test

The acute toxicity profiles of MeOH-AI have been studied in Swiss albino mice. When administered orally at a single dose of 500–4000 mg/kg, MeOH-AI did not cause any toxicity or mortality in the experimental mice. No evidence of behavioral toxicity was detected in experimental animals during 72 h of post-treatment. This study concluded that MeOH-AI has a median lethal dose (LD_{50}) value greater than 4000 mg/kg, implying that it is virtually safe to use. Hence, based on this study, dose levels of 200 and 400 mg/kg b.w. were determined for the current in vivo experiments.

3.4. Antidepressant effects of MeOH-AI

3.4.1. Tail suspension test

The TST was used to measure antidepressive activity test, following the oral administration of 200 and 400 mg/kg MeOH-AI. The results are shown in Fig. 2**.** In TST, mice treated with MeOH-AI at doses of 200 and 400 mg/kg demonstrated a 46.98% (immobility time: 85.00 ± 7.64 s; $p < 0.01$) and 22.45% (immobility time: 124.33 ± 5.04 s; $p > 0.05$) reduction in immobile state, respectively, compared to the NC group

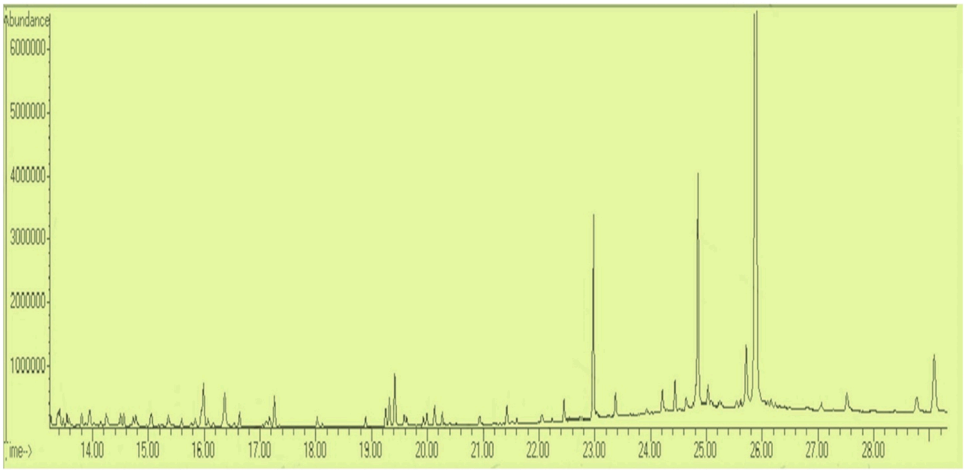

Fig. 1. Total ionic chromatogram (TIC) of the methanol extract of whole-plant of *A. indica* using gas chromatography-mass spectrometry (GC–MS).

(immobility time: 160.33 ± 1.45 s). Interestingly, mice given the standard drug (imipramine HCl at 10 mg/kg) showed a 46.57% (immobility time: 85.66 ± 2.03 s; $p < 0.01$ vs. NC group) reduction in immobility time, which is nearly equal to the 400 mg/kg dose of MeOH-AI. These results indicate that MeOH-AI at a 400 mg/kg dose exerts strong and significant antidepressant-like effects.

3.4.2. Forced swim test

The FST was also used to measure antidepressive activity, following the oral administration of 200 and 400 mg/kg MeOH-AI, shown in Fig. 3**.** As seen in the figure, administration of MeOH-AI at 400 mg/kg significantly decreased ($p < 0.01$) the immobility time of mice by 17.47% (immobility time: 97.66 ± 1.45 s) compared to the NC group (immobility time: 118.33 ± 1.20 s). However, the 200 mg/kg dose of MeOH-AI did not exert any noticeable effect on the experimental animals. As anticipated, the mouse group treated with the reference control imipramine (10 mg/kg) demonstrated a maximum reduction of 25.35% in the immobility period (immobility time: 88.33 ± 0.88 s; $p < 0.01$) compared to the NC group.

3.5. Antidiarrheal activity of MeOH-AI

3.5.1. Castor oil-induced diarrhea

The castor oil-induced diarrhea model showed that MeOH-AI administration resulted in the significant inhibition of diarrhea in a dose-dependent manner, displayed in Table 3**.** A stronger inhibitory effect was observed for the 400 mg/kg dose (81.77 ± 3.44%), which was similar to the inhibitory effect induced by the reference drug, loperamide (82.77 ± 0.29%). MeOH-AI also demonstrated inhibitory effects at the 200 mg/kg dose (65.27 ± 1.54%). These results indicate that MeOH-AI possesses significant ($p < 0.01$) antidiarrheal activity against castor oil-induced diarrhea when compared to the NC group.

3.5.2. Gastrointestinal motility

The gastrointestinal (GI) motility assay indicated that MeOH-AI treatment significantly inhibited diarrhea in the experimental mice, showed in Fig. 4**.** A significant inhibitory effect ($p < 0.01$) was observed for the 400 mg/kg dose (64.60 ± 5.51%) when compared with the NC group, which was stronger than the effect observed for the reference drug, loperamide (42.36 ± 0.69%). MeOH-AI also demonstrated an inhibitory effect at the 200 mg/kg dose (49.09 ± 2.43%). These results indicate that MeOH-AI possesses good antidiarrheal activity.

3.6. Anti-inflammatory effects of MeOH-AI

3.6.1. Inhibition of protein denaturation

Anti-inflammatory activity was assessed by examining the protein denaturation of BSA. The results, shown in Fig. 5, demonstrated the significant ($p < 0.05$) inhibition of protein denaturation by MeOH-AI, and anti-inflammatory activity increased in a concentration-dependent manner. MeOH-AI showed 43.07 ± 0.42%, 49.39 ± 0.48%, 54.49 ± 0.42%, 62.77 ± 0.42%, and 79.80 ± 0.64% denaturation inhibition at concentrations of 31.25, 62.5, 125, 250, and 500 μg/mL, respectively. By comparison, the standard drug diclofenac sodium showed a maximum denaturation inhibition of 67.85 ± 0.34% at a concentration of 500 μg/mL.

3.6.2. Heat-induced hemolysis

Anti-inflammatory activity was analyzed using an erythrocyte suspension under conditions of heat-induced hemolysis. The results, as shown in Fig. 6**,** demonstrated the significant ($p < 0.05$) inhibition of hemolysis by MeOH-AI. The anti-inflammatory activity of MeOH-AI, as measured by the percent inhibition of hemolysis, increased in a concentration-dependent manner. The methanol extract demonstrated hemolysis inhibitory activities of 64.32 ± 0.52%, 67.12 ± 0.28%, 74.87 ± 0.42%, and 83.24 ± 0.64%, at concentrations of 250. 500, 1000, and 2000 μg/mL, respectively, whereas the standard drug acetyl salicylic acid showed a maximum hemolysis inhibition of 134.48 ± 0.84% at a concentration of 2000 μg/mL.

3.6.3. Hypotonic solution–induced hemolysis

Anti-inflammatory activity was analyzed using an erythrocyte suspension under conditions of a hypotonic solution–induced hemolysis. The results, shown in Fig. 7**,** demonstrated the significant ($p < 0.05$ and $p < 0.01$) inhibition of hemolysis by MeOH-AI, which increased in a concentration-dependent manner. MeOH-AI demonstrated hemolysis inhibitory activities of 15.63 ± 0.46%, 21.70 ± 0.58%, 36.86 ± 0.38%, 42.30 ± 0.35%, and 53.54 ± 2.71% at concentrations of 31.25, 62.5, 125, 250, and 500 μg/mL, respectively, compared with diclofenac sodium, the standard reference drug, which showed a maximum inhibitory effect at a 500 μg/mL concentration.

3.7. Thrombolytic effect of MeOH-AI

The thrombolytic activity of MeOH-AI is shown in Fig. 8. MeOH-AI significantly ($p < 0.01$) induced 19.19% lysis in the blood clot, compared with 48.82% by the positive control, streptokinase, and 8.33% by the negative control, water.

Table 1
Chemical compounds identified from the *A. indica* methanolic extract using gas chromatography-mass spectrometry (GC-MS) analysis.

Sl. no.	Name of identified compounds	R. T.	Peak area (%)
1	3-Quinolinecarboxylic acid, 6,7-difluoro-1,4-dihydro-4-oxo-, ethylester	5.378	0.779
2	2,3-Dihydro-5-[4E)− 3-hydroxy-4-methyl-6-(2,6,6-trimethylcyclohexenyl)− 4-hexene	7.833	0.353
3	6-Aza-5,7,12,14-tetrathiapentacene	10.047	0.434
4	3-Ethylthio-2-hydroxy-2-methyl-N-phenyl-1,4-dioxane-3-carboxamide	10.110	0.459
5	Phenol, 2,4-Bis(1,1-Dimethylethyl)− 2,4-Ditert-Butylphenol	11.895	0.363
6	7-Fluoro-3-(5,6,78-tetrahydro-1-naphthalenyl)− 1(3 H)-isobenzofuranone	12.136	0.768
7	2(4 H)-Benzofuranone, 5,6,7,7a-tetrahydro-4,4,7a-trimethyl	12.359	0.397
8	3-Hydroxy-beta-damascone	13.212	0.095
9	1-Methylcycloheptanol	13.377	0.601
10	Butenol, methyl- (CAS)	13.475	0.289
11	2-Cyclohexen-1-one, 4-(3-hydroxy-1-butenyl)− 3,5,5-trimethyl-, [R-[R* ,R* -(E)]]-	13.578	0.414
12	N-Ethoxy-4-methyl-5-(p-methoxyphenyl) thiazole-2(3 H)-thione	13.950	0.844
13	6-Methyl-2,3-dihydropyran-2,4-dione	14.144	0.235
14	(+)-Isololiolide	14.779	0.576
15	Pluchidiol	15.357	0.623
16	Neophytadiene-7,11,15-Trimethyl, 3-Methylene-1-Hexadecene	15.987	2.473
17	2-Pentadecanone, 6,10,14-trimethyl-Hexahydro-farnesyl acetone	16.072	0.310
18	2-Hexadecen-1-ol, 3,7,11,15-tetramethyl-, [R-[R* ,R* -(E)]]- (CAS)	16.633	0.580
19	Bicyclo[8.1.0] undecane	16.364	2.104
20	Hexadecanoic acid, methyl ester	17.257	1.176
21	3,4-Dihydro-3-methyl-1-phenylquinolin-2(1 H)-one	18.024	0.406
22	Hexadecanoic acid, ethyl ester	18.121	0.134
23	3,4-Dihydro-3-methyl-1-phenylquinolin-2(1 H)-one	19.254	0.636
24	Hexadecanoic acid, ethyl	19.323	1.108
25	9,12-Octadecadienoic acid (*Z,Z*)-, methyl ester	19.420	2.233
26	cis-13-Octadecenoic acid, methyl ester	19.586	0.406
27	2-Hexadecen-1-ol, 3,7,11,15-tetramethyl-, [R-[R* ,R* -(E)]]- (CAS)	19.632	0.417
28	Octadecanoic acid, methyl ester Stearic acid, methyl ester Kemester	19.929	0.301
29	1-(2-Phenoxyethyl)− 1 H-indole	19.992	0.463
30	Ethyl linoleate	20.129	0.846
31	Ethyl oleate	20.404	0.135
32	1-Thienylcyclohexene	20.942	0.406
33	2-Mercapto-4-methoxypyridine-1-oxide-4-methoxy-2-pyridinethiol 1-oxide	21.606	0.127
34	3,4-Dihydro-3-methyl-1-phenylquinolin-2(1 H)-one	22.241	0.207
35	2(3 H)-Furanone, 5-hexyldihydro-4-methyl-, trans-(+)-	22.550	0.0714
36	2-Methyl-5 H-dibenz[*b,f*]azepine	24.638	1.569
37	1 H-Indole-2-carboxylic acid, 6-(4-ethoxyphenyl)− 3-methyl-4-oxo-4,5,6,7-tetra	24.770	0.622
38	Ethane, 1-(4,4,4-trifluoro-1,3-dithiobutyl)− 2-(3,3,3-trifluoro-1,2-dithiopro	24.850	10.394
39	N-Cyano-N′,N’,N’’,N′’-tetramethyl-1,3,5-triazinetriamine	24.959	0.831
40	2,6,10,14,18,22-Tetracosahexaene, 2,6,10,15,19,23-hexamethyl-, (all-E)-	25.245	1.839
41	5-Chloro-2-phenyloxazole-4-carbaldehyde	25.720	4.556
42	2-(4-Methylphenyl)ethynylaniline	25.891	46.539
43	4-Dehydroxy-N-(4,5-methylenedioxy-2-nitrobenzylidene)tyramine	27.522	1.669
44	Alpha-Humulene	29.084	3.964
45	Vitamin E	5.3786	0.779
46	Stigmasterol	7.8333	0.353

R.T.: Retention time.

3.8. *In silico study*

3.8.1. *Molecular docking*

In the current study, we applied a molecular docking model to examine the docking of 12 selected compounds detected in MeOH-AI by the GC–MS analysis with several target proteins involved in inflammation (COX-2), thrombosis (TPA), depression (SERT3, MAO-A), and diarrhea (M3MACR, 5-HT3 receptor). The docking values of the compounds are listed in Table 4, and key binding interactions with the active site residues of the tested proteins are shown in Figs. (9–11) and supplementary Figs. S1-S3.

3.8.2. *Molecular docking study for anti-inflammatory activity*

COX-2 (PDB ID: 4PH9) mediates the anti-inflammatory effects of non-steroidal anti-inflammatory drugs and was included in this docking study to investigate the potential underlying anti-inflammatory mechanisms of MeOH-AI at the molecular level. Among the compounds that were studied, 4-dehydroxy-N-(4,5-methylenedioxy-2-nitrobenzylidene) tyramine exhibited the highest binding energies with COX-2, featuring a docking score of −7.725 kcal/mol, whereas the standard anti-inflammatory drug (diclofenac sodium) demonstrated a slightly higher binding energy (docking score of −7.814 kcal/mol). The strength of the interactions between COX-2 and the tested compounds, in order according to docking score, was as follows: diclofenac sodium > 4-dehydroxy-N-(4,5-methylenedioxy-2-nitrobenzylidene)tyramine > ethane, 1-(4,4,4-trifluro-1,3-dithiobutyl)− 2-(3,3,3-trifluoro-1,2-dithiopropyl)- > 2,6,10,14,18,22-tetracosahexaene, 2,6,10,15,19,23-hexamethyl-, (all-E)- > 2-(4-methylphenyl)ethynylaniline > 2-hexadecen-1-ol, 3,7,11,15-tetramethyl-, [R-[R* ,R* -(E)]]- > hexadecanoic acid, methyl ester > neophytadiene > cis-13-octadecenoic acid, methyl ester. However, two of the identified compounds, stigmasterol and vitamin E, did not dock against COX-2. An in-depth analysis of the protein-ligand complexes exposed a range of binding interactions between the active site residues of the target enzyme and the studied compounds. The strongest interaction, between 4-dehydroxy-N-(4,5-methylenedioxy-2-nitrobenzylidene) tyramine and COX-2, involved the formation of two H-bond interactions with Arg121 and Tyr356 and seven hydrophobic interactions with Trp388 (pi-pi t-shaped), Val117 (alkyl), Arg121 (alkyl), Ala528 (alkyl), Val350 (pi-alkyl), Tyr356 (pi-alkyl), and Ala528 (pi-alkyl), in Fig. 9**A**. By contrast, the interaction between diclofenac sodium and COX-2 involved the formation of one H-bond with Tyr356 and five hydrophobic (pi-alkyl) interactions with Val350, Leu353, Val524, Ala528, and Leu532 shown in Fig. S1A.

3.8.3. *Molecular docking study for thrombolytic activity*

The compounds were docked against TPA (PDB ID: 1A5H) to elucidate the possible molecular mechanisms underlying the thrombolytic effects of MeOH-AI. An analysis of the docking scores revealed that stigmasterol possessed the most favorable binding affinity with TPA among the tested compounds (docking score −5.851 kcal/mol), although streptokinase (the standard thrombolytic medication) possessed the strongest binding affinity (docking score −6.672 kcal/mol). Based on the docking scores, the affinities of the tested compounds and streptokinase for TPA could be ranked as follows: streptokinase > stigmasterol > 4-dehydroxy-N-(4,5-methylenedioxy-2-nitrobenzylidene) tyramine > ethane, 1-(4,4,4-trifluro-1,3-dithiobutyl)− 2-(3,3,3-trifluoro-1,2-dithiopropyl)- > 2-(4-methylphenyl)ethynylaniline > vitamin E > 2,6,10,14,18,22-tetracosahexaene, 2,6,10,15,19,23-hexamethyl-, (all-E)- > 2-hexadecen-1-ol, 3,7,11,15-tetramethyl-, [R-[R* ,R* -(E)]]- > neophytadiene > cis-13-octadecenoic acid, methyl ester > hexadecanoic acid, methyl ester. An in-depth visualization of the receptor-ligand complex structures revealed that stigmasterol bound to the active site of TPA protein via two H-bond interactions with Arg39 and Glu60A and six hydrophobic interactions with Leu41 (alkyl), Cys42 (alkyl), Cys220 (alkyl), His57 (pi-sigma), His57 (pi-alkyl), and Tyr99 (pi-alkyl), exhibited in Fig. 9B. By comparison, streptokinase bound to

Table 2
Concentration of some chemical elements and physical parameters in *A. indica*.

Chemical elements	Concentration (mg/kg)	Chemical elements	Concentration (mg/kg)	Physical parameters	Content (%)
Cd	0.47	Zn	72.12	Moisture	10.04
Mn	21.73	Ca	2379.97	Ash	3.03
Co	0.52	Mg	2832.68	OMC	96.97
Ni	19.92	K	4791.36		
Cu	7.55	P	1890.39		
Fe	156.25				

OMC Organic matter content.

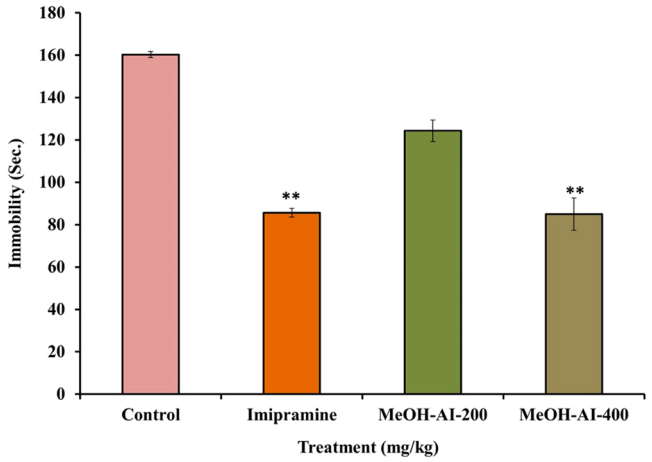

Fig. 2. Antidepressant activity of whole-plant MeOH-AI measured using the tail suspension model. Values are expressed as the mean ± SEM (n = 6), * *p < 0.01 and *p < 0.05. MeOH-AI = methanol extract of *Anisomeles indica*.

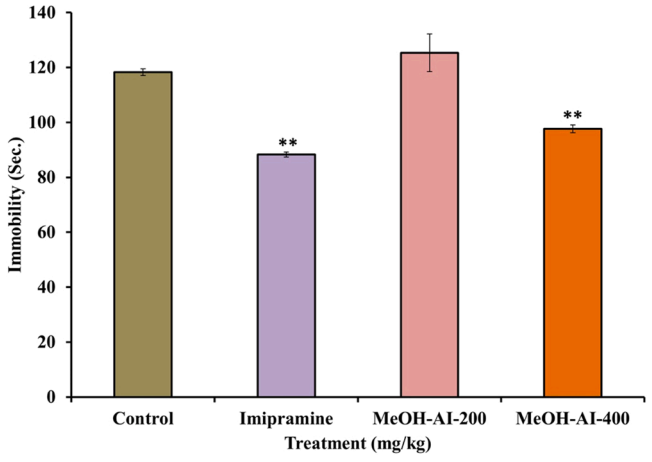

Fig. 3. Antidepressant activity of whole-plant MeOH-AI measured using the forced swim model. Values are expressed as the mean ± SEM (n = 6). * *p < 0.01 and *p < 0.05. MeOH-AI = methanol extract of *Anisomeles indica*.

the same protein through the formation of two H-bond interactions with Asp97 and Thr175 and one hydrophobic interaction with Tyr99 (pi-alkyl) in Fig. S1B.

3.8.4. Molecular docking study for antidepressant activity

The docking study performed to explore the molecular mechanisms of the observed antidepressant effect targeted two key proteins involved in the monoaminergic system: SERT3 and MAO-A. For binding with SERT3 (PDB ID: 5I6X), 2-(4-Methylphenyl)ethylaniline demonstrated the best docking score of − 7.888 kcal/mol compared with the docking score of − 9.426 kcal/mol for fluoxetine, a commonly prescribed

Table 3
Effects of MeOH-AI on the frequency of defecation of diarrheal induction in castor oil-induced diarrheal mice.

Group	Treatment	Total number of feces	% of inhibition
	Castor oil + saline (2 mg/kg)	30.66 ± 0.88	-
	Castor oil + loperamide (5 mg/kg)	5.16 ± 0.08 * *	82.77 ± 0.29
	Castor oil + MeOH-AI (200 mg/kg)	10.41 ± 0.46 * *	65.27 ± 1.54
	Castor oil + MeOH-AI (400 mg/kg)	5.41 ± 1.02 * *	81.77 ± 3.44

The values are presented as mean ± SEM (n = 6), where SEM = Standard error mean. * *p < 0.01 indicates statistically significant compared to the negative control group.

selective serotonin reuptake inhibitor. According to the strength of the docking scores for SERT3, the tested compounds could be ranked in the following order: 4-dehydroxy-N-(4,5-methylenedioxy-2-nitrobenzylidene)tyramine > 2,6,10,14,18,22-tetracosahexaene, 2,6,10,15,19,23-hexamethyl-, (all-E)- > vitamin E > stigmasterol > ethane, 1-(4,4,4-trifluro-1,3-dithiobutyl)− 2-(3,3,3-trifluoro-1,2-dithiopropyl)- > 2-hexadecen-1-ol, 3,7,11,15-tetramethyl-, [R-[R* ,R* -(E)]]- > cis-13-octadecenoic acid, methyl ester > neophytadiene > hexadecanoic acid, methyl ester. The positioning of the ligands with the SERT3 binding site revealed that 2-(4-methylphenyl)ethylaniline formed two H-bond interactions with Tyr95 and Ser438 and seven hydrophobic interactions with Tyr95 (pi-pi stacked), Tyr176 (pi-pi t-shaped), Ser438 (amide-pi stacked), Ala173 (alkyl), Leu443 (alkyl), Ile172 (pi-alkyl), and Ala173 (pi-alkyl), shown Fig. 10A. By comparison, fluoxetine formed one H-bond interaction with Tyr95 and seven hydrophobic interactions with Tyr176 (pi-pi t-shaped), Phe341 (pi-pi t-shaped), Ile172 (alkyl), Ala173 (alkyl), Ile172 (two pi-alkyl interactions), and Val501 (pi-alkyl), exposed in Fig. S2A.

The compounds were then docked with MAO-A (PDB ID: 2Z5Y), and the results are shown in Table 4. The docking analysis demonstrated that 4-dehydroxy-N-(4,5-methylenedioxy-2-nitrobenzylidene)tyramine exerted the optimal binding affinity for MAO-A, with a docking score of − 8.832 kcal/mol, followed by 2-(4-methylphenyl)ethynylaniline (docking score of −7.888 kcal/mol), ethane, 1-(4,4,4-trifluro-1,3-dithiobutyl)− 2-(3,3,3-trifluoro-1,2-dithiopropyl)- (docking score of −6.558 kcal/mol), and 2,6,10,14,18,22-tetracosahexaene, 2,6,10,15,19,23-hexamethyl-, (all-E)- (docking score of −6.006 kcal/mol). Surprisingly, the docking score for the reference MAO-A inhibitor phenelzine was ascertained to be − 6.782 kcal/mol, which is significantly lower than the scores obtained for 4-dehydroxy-N-(4,5-methylenedioxy-2-nitrobenzylidene) tyramine and 2-(4-methylphenyl) ethynylaniline. However, three compounds (α-humulene, vitamin E, and stigmasterol) demonstrated no affinity for MAO-A. Investigating the orientation of the tested compounds and phenelzine at the substrate-binding site of the MAO-A enzyme revealed a variety of ligand–residue interactions. The best-scored compound, 4-dehydroxy-N-(4,5-methylenedioxy-2-nitrobenzylidene)tyramine, bound to the enzymatic pocket of MAO-A by forming two H-bond interactions with Ala68 and Tyr69 and six hydrophobic interactions with Tyr407 (pi-pi stacked),

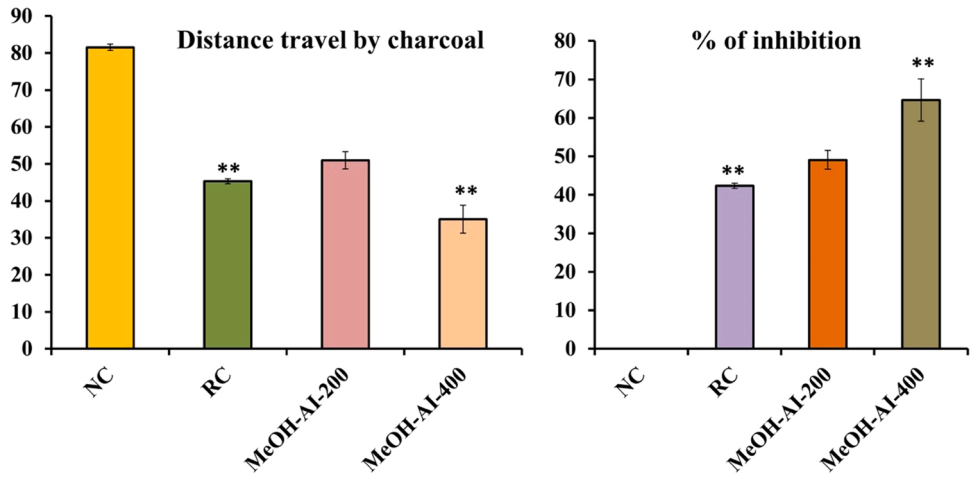

Fig. 4. Antidiarrheal activity evaluation measured using the GI motility test. Values are expressed as the mean ± SEM (n = 6). * *p < 0.01 and *p < 0.05, significant compared with control. RC = Reference control, loperamide, NC = negative control, saline, MeOH-AI = methanol extract of *Anisomeles indica*.

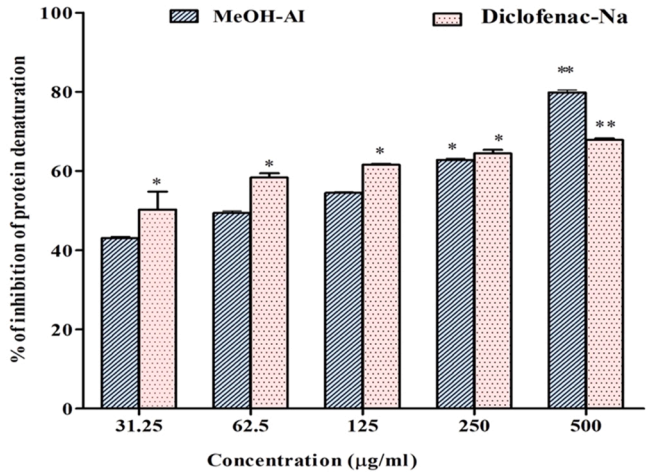

Fig. 5. Percentage inhibition of protein denaturation by MeOH-AI. Results represent the mean ± SEM (n = 3). *p < 0.05, significantly different compared with control. MeOH-AI = methanol extract of *Anisomeles indica*.

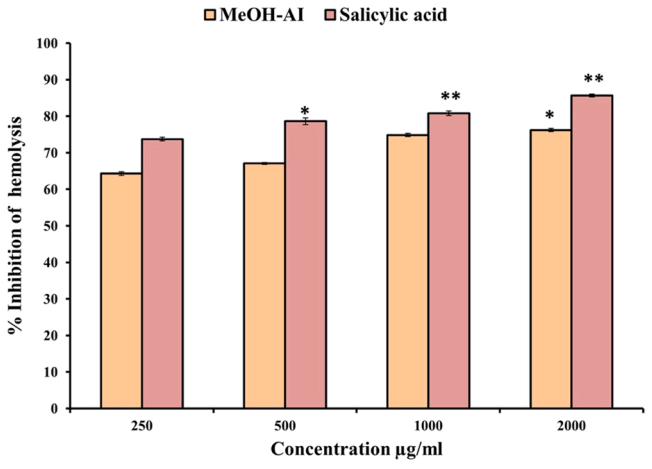

Fig. 6. Anti-inflammatory activity of whole-plant MeOH-AI as assessed using a heat-induced hemolysis model. Values are expressed as the mean ± SEM (n = 3). * *p < 0.01 and *p < 0.05, significant relative to control. MeOH-AI = methanol extract of *Anisomeles indica*.

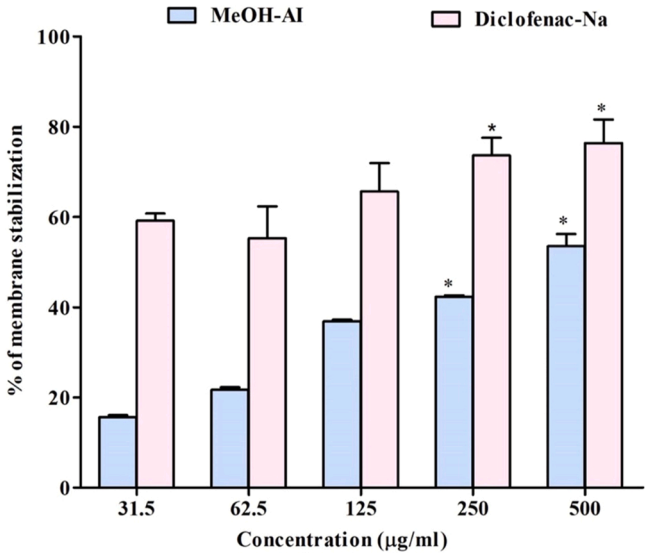

Fig. 7. Percentage inhibition of hypotonic solution–induced hemolysis of the erythrocyte membrane by MeOH-AI and standard drug. Values are presented as the mean ± SEM (n = 3). *p < 0.05, significantly different compared with control. MeOH-AI = methanol extract of *Anisomeles indica*.

Arg51 (amide-pi stacked), Tyr444 (amide-pi stacked), Arg51 (pi-alkyl), Tyr407 (pi-alkyl), and Ala448 (pi-alkyl), in Fig. 10**B**; whereas the next best compound, 2-(4-methylphenyl)ethynylaniline, bound to MAO-A by forming one H-bond interaction with Asn181 and two hydrophobic interactions with Tyr407 (pi-pi stacked), and Ile180 (pi-alkyl) as in Fig. 10**C.** Phenelzine interacted with the same target enzyme by establishing three H- bond interactions with Ile180, Asn181, and Gln215 and three hydrophobic (pi-alkyl) interactions with Ile335, Leu337, and Tyr407, noted in Fig. S2B.

3.8.5. Molecular docking study for antidiarrheal activity

To clarify the antidiarrheal effects of MeOH-AI in the docking study, the compounds were docked against two main receptors, M3MACR, and 5-HT3 receptor, which are involved in the underlying molecular mechanism that regulates intestinal motility. In the case of M3MACR (PDB ID: 4U14), an analysis of the docking scores indicated that 4-dehydroxy-N-(4,5-methylenedioxy-2-nitrobenzylidene)tyramine and vitamin E demonstrated the best binding energies with M3MACR, with docking scores of − 10.41 and − 9.206 kcal/mol, respectively,

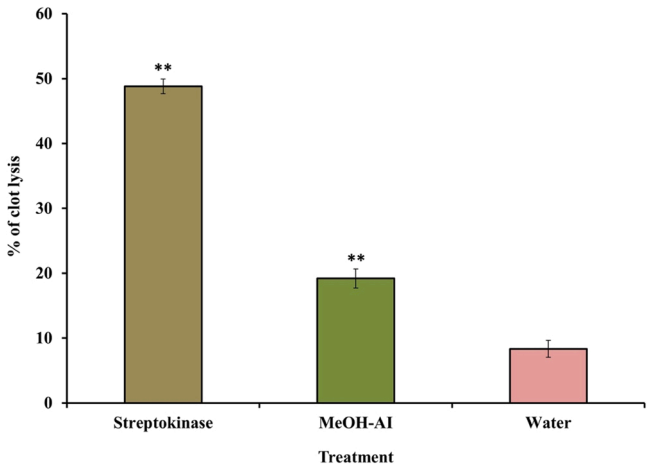

Fig. 8. Thrombolytic study by clot lysis test. Effects of water, MeOH-AI, and streptokinase on the dissolution of clots prepared from the blood of normal individuals. Values are expressed as the mean ± SEM (n = 7). * *p < 0.01 and *p < 0.05, were considered significant different compared with control. MeOH-AI = methanol extract of *Anisomeles indica.*

followed by α-humulene and 2-(4-methylphenyl)ethynylaniline (docking scores of −7.936 and −7.108 kcal/mol, respectively). The established antidiarrheal drug loperamide manifested a docking score of − 8.543 kcal/mol. In addition, stigmasterol was found to have no affinity for M3MACR. A molecular analysis of the receptor-ligand complexes revealed that 4-dehydroxy-N-(4,5-methylenedioxy-2-nitrobenzylidene)tyramine interacted with the substrate-binding site of M3MACR via the formation of two H-bond interactions with Ser151 and Asn507 and nine hydrophobic interactions with Trp503 (pi-pi stacked), Tyr529 (pi-pi stacked), Tyr506 (pi-pi t-shaped), Cys532 (alkyl), Ala235 (pi-alkyl), Ala238 (pi-alkyl), Tyr529 (pi-alkyl), Cys532 (pi-alkyl), and Tyr533 (pi-alkyl) in Fig. 11A; vitamin E interacted through the formation of one H-bond interaction with Ser151 and nineteen hydrophobic interactions with Tyr148 (pi-pi stacked), Leu144 (alkyl), Leu225 (three alkyl interactions), Ala235 (alkyl), Ala238 (alkyl), Phe124 (pi-alkyl), Trp143 (pi-alkyl), Tyr148 (two pi-alkyl interactions), Trp199 (pi-alkyl), Trp503 (pi-alkyl), Tyr506 (two pi-alkyl interactions), Trp525 (two pi-alkyl interactions), and Tyr529 (two pi-alkyl interactions), exposed in Fig. 11B. By contrast, loperamide bound to M3MARC by forming two H-bond interactions with Thr231 and Tyr506 and ten hydrophobic interactions with Tyr148 (pi-pi stacked), Trp525 (pi-pi stacked), Tyr506 (pi-pi t-shaped), Cys532 (alkyl), Trp503 (pi-sigma), Ala238 (pi-alkyl), Trp503 (pi-alkyl), Tyr506 (pi-alkyl), Trp525 (pi-alkyl), and Cys532 (pi-alkyl), showed in Fig. S3A.

4-Dehydroxy-N-(4,5-methylenedioxy-2-nitrobenzylidene) tyramine was also found to display a substantially higher affinity for the 5-HT3 receptor (PDB ID: 5AIN) than the reference standard alosetron. The 5HT3 receptor is another key therapeutic target protein for the design of antidiarrheal drugs. For the 5-HT3 receptor, the docking score of 4-dehydroxy-N-(4,5-methylenedioxy-2-nitrobenzylidene) tyramine was computed to be − 7.491 kcal/mol, whereas alosetron generated a weaker docking score of − 6.621 kcal/mol. Based on the docking scores, the strength of the binding affinities against 5HT-3 receptor for the examined compounds can be ranked as follows: 4-dehydroxy-N-(4,5-methylenedioxy-2-nitrobenzylidene) tyramine > alosetron > ethane, 1-(4,4,4-trifluro-1,3-dithiobutyl)− 2-(3,3,3-trifluoro-1,2-dithiopropyl)- > 2-(4-methylphenyl)ethynylaniline > vitamin E > 2-hexadecen-1-ol, 3,7,11,15-tetramethyl-, [R-[R* ,R* -(E)]]- > 2,6,10,14,18,22-tetracosahexaene, 2,6,10,15,19,23-hexamethyl-, (all-E)- > stigmasterol > cis-13-octadecenoic acid, methyl ester > neophytadiene > hexadecanoic acid, methyl ester. Analysis of the receptor–ligand interactions revealed that the best-scored compound, 4-dehydroxy-N-(4,5-methylenedioxy-2-nitrobenzylidene) tyramine, bound to the active site of the 5-HT3 receptor through the formation of three H-bond interactions with Ile116, Trp145, and Cys188 and twelve hydrophobic interactions with Tyr53 (pi-pi t-shaped), Val106 (alkyl), Met114 (alkyl), Val146 (alkyl), Cys189 (alkyl), Val146 (pi-sigma), Met114 (pi-alkyl), Ile116 (two pi-alkyl interactions), Cys188 (two pi-alkyl interactions), and Cys189 (pi-alkyl) in Fig. 11C. However, alosetron interacted to the binding site of the same receptor through the formation of one H-bond interaction with Asp162 and sixteen hydrophobic interactions with Trp145 (pi-pi t-shaped), Ile116 (two alkyl interactions), Val116 (alkyl), Tyr53 (two pi-alkyl interactions), Met114 (pi-alkyl), Ile116 (two pi-alkyl interactions), Trp145 (two pi-alkyl interactions), Val146 (two pi-alkyl interactions), Tyr186 (pi-alkyl) Cys188 (pi-alkyl), and Cys189 (pi-alkyl), reported in Fig. S3B.

3.8.6. *PASS-predicted activity spectrum*

Table 5 shows the prediction of activity spectra for substances (PASS)-based biological activities of the eight top-ranked compounds identified by the docking studies. PASS analysis revealed that 2,6,10,14,18,22-tetracosahexaene, 2,6,10,15,19,23-hexamethyl-, (all-E)-; stigmasterol; and vitamin E possess the promising potential to exert anti-inflammatory activity, with probability of activity (Pa) values

Table 4
Docking scores of the assigned compounds from MeOH-AI and reference standard drug against COX-2 for anti-inflammatory activity, TPA for thrombolytic activity, SERT3 and MAO-A for antidepressant activity, and M3MACR and 5-HT3 receptor for antidiarrheal activity.

Proteins	COX-2	TPA	SERT3	MAO-A	M3MACR	5-HT3
PDB Codes	4PH9	1A5H	5I6X	2Z5Y	4U14	5AIN
Compounds	Docking Scores (kcal/mol)					
Alpha-Humulene	− 6.319	− 5.236	− 6.387	–	− 7.936	− 5.752
2TCH2H	− 5.779	− 3.302	− 6.275	− 6.006	− 6.933	− 2.909
4DHNT	− 7.725	− 5.729	− 6.687	**− 8.832**	**−10.41**	**−7.491**
Stigmasterol	–	− 5.851	− 5.86	–	–	− 2.63
Neophytadiene	− 2.291	− 1.692	− 1.867	− 3.983	− 3.606	− 0.511
2HD3T	-3.4	− 2.113	− 3.788	− 4.996	− 4.242	− 3.307
Bicyclo[8.1.0]undecane	− 7.118	− 5.838	− 5.891	− 6.311	− 6.868	− 5.269
2-(4-Methylphenyl)ethynylaniline	− 5.742	− 3.999	− 7.818	− 7.888	− 7.108	− 5.552
Vitamin E	–	− 3.941	− 5.901	–	− 9.206	− 4.64
E12TD	− 6.703	− 4.15	− 5.611	− 6.558	− 6.64	− 5.824
Hexadecanoic acid, methyl ester	− 3.008	− 0.243	− 0.497	− 2.129	− 2.058	0.032
cis-13-Octadecenoic acid, methyl ester	− 1.119	− 1.363	− 1.916	− 3.589	− 3.264	− 0.678
Reference standard	**−7.814**	**−6.672**	**−9.426**	− 6.782	− 8.543	− 6.621

Bold text represents the highest score. 2TCH2H: 2,6,10,14,18,22-Tetracosahexaene, 2,6,10,15,19,23-hexamethyl-, (all-E)-; 4DHNT: 4-Dehydroxy-N-(4,5-methylenedioxy-2-nitrobenzylidene)tyramine; 2HD3T: 2-Hexadecen-1-ol, 3,7,11,15-tetramethyl-, [R-[R* ,R* -(E)]]-; E12TD: Ethane, 1-(4,4,4-trifluro-1,3-dithiobutyl)− 2-(3,3,3-trifluoro-1,2-dithiopropyl)-; Reference Standard: Diclofenac (COX-2), Streptokinase (TPA), Fluoxetine (SERT3), Phenelzine (MAO-A), Loperamide (M3MACR), and Alosetron (5-HT3).

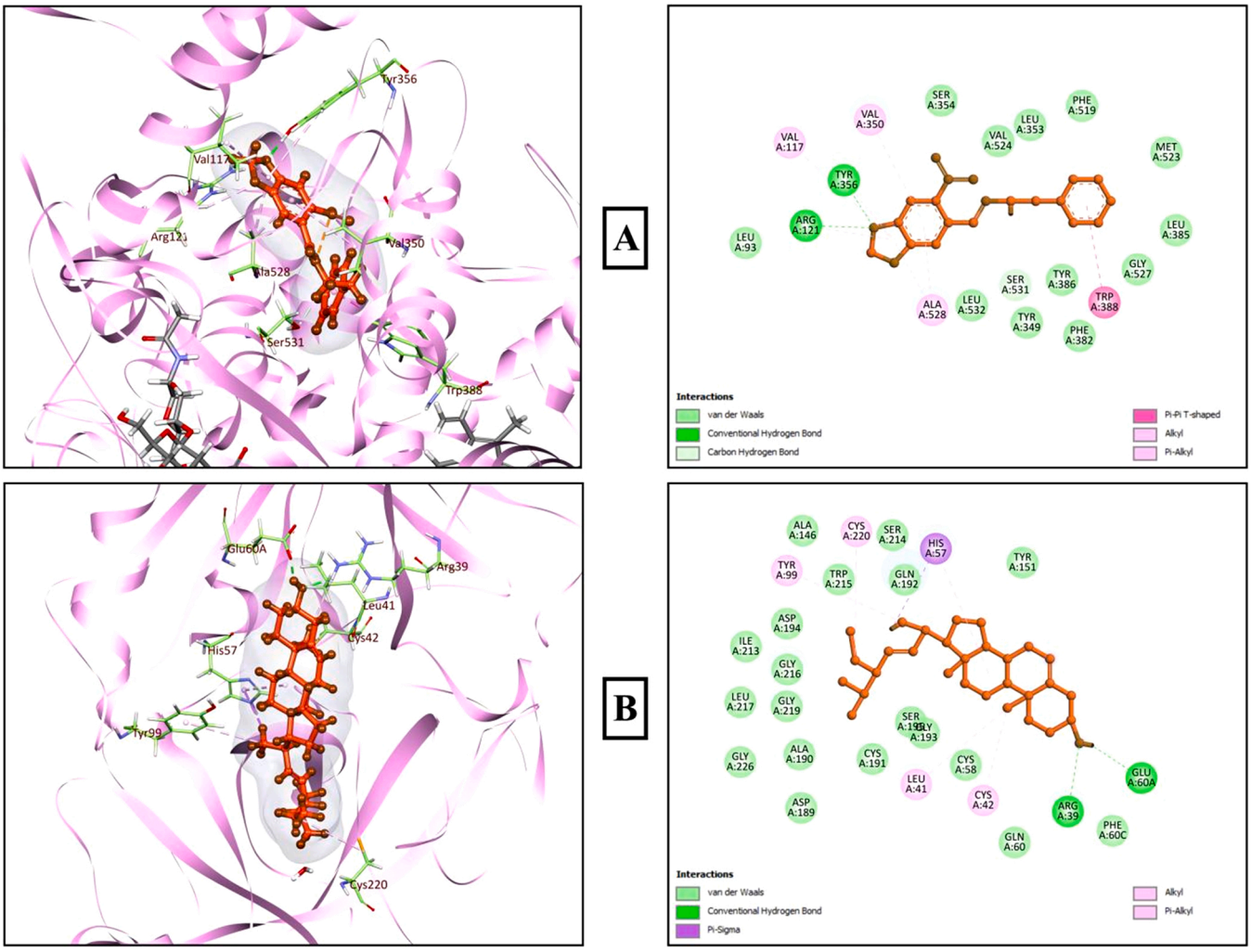

Fig. 9. Best-ranked docking poses (left) and 2D visualizations of the interactions (right) between (A) 4-dehydroxy-N-(4,5-methylenedioxy-2-nitrobenzylidene)tyramine and the active site residues of COX-2 (PDB ID: 4PH9) and between (B) stigmasterol and the active site residues of TPA (PDB ID: 1A5H).

ranging from 0.0542 to 0.814. The compounds α-humulene; 2,6,10,14,18,22-tetracosahexaene, 2,6,10,15,19,23-hexamethyl-, (all-E)-; are likely to act as potent fibrinolytic/thrombolytic/antithrombotic agents (Pa values ranging from 0.503 to 0.734). PASS also predicted that 4-dehydroxy-N-(4,5-methylenedioxy-2-nitrobenzylidene) tyramine might potentially inhibit neurotransmitter uptake (Pa values of0.739 and 0.637, respectively). In addition, the PASS analysis of the test compounds disclosed several possible targets for mitigating inflammation, thrombosis, depressive disorders, and diarrhea.

3.8.7. *ADME/T profiles*

Table 6 presents the drug-like characteristics of potentially bioactive metabolites identified in MeOH-AI, describing the physiochemical properties established by Lipinski's rule of five (RoF) and Veber's rules. As shown in Table 6, the physicochemical properties of the compounds studied were within acceptable limits in most cases, and none of the studied compounds violated more than one Lipinski rule. The pharmacokinetic and toxicity (ADME/T) properties are provided in Table 7. Caco-2 permeability, human intestinal absorption (%), and P-gp substrate were used to determine the degree of absorption. All compounds are expected to have high Caco-2 permeability and intestinal absorption, with values predicted in the range of 1.216–1.516% and 85.75%–94.97%, respectively. The results also indicated that the compounds 2,6,10,14,18,22 tetracosahexaene, 2,6,10,15,19,23-hexamethyl-; 4-dehydroxy-N-(4,5-methylenedioxy-2-nitrobenzylidene) tyramine; stigmasterol; and vitamin E are all not P-gp substrates. The projected values for the volume of distribution at steady state (VDss) ranged from − 0.058–0.709, suggesting that most of the studied compounds are expected to have favorable distribution volumes. The compounds were predicted to readily cross the blood-brain barrier (BBB; logBB values ranging from −0.515 to 0.771). Additionally, the brain permeation (logPS) values for the compounds were computed to range from − 2.734 to − 0.955, indicating that the compounds 2,6,10,14,18,22-tetracosahexaene, 2,6,10,15,19,23-hexamethyl-, (all-E)-; stigmasterol; 2-(4-methylphenyl)ethynylaniline; and vitamin E would easily penetrate the central nervous system (CNS). The metabolism profile suggested that 2,6,10,14,18,22-tetracosahexaene, 2,6,10,15,19,23-hexamethyl-, (all-E)-; stigmasterol; were unlikely to inhibit any cytochrome P (CYP) enzymes; by contrast, vitamin E and ethane, 1-(4,4,4-trifluro-1,3-dithiobutyl)− 2-(3,3,3-trifluoro-1,2-dithiopropyl)- were expected to inhibit CYP2C19. The estimated total clearance of the compounds ranged from 0.618 to 1.791 mL/min/kg, and all compounds were predicted to be renal organic cation transporter 2 (OCT2) non-substrates. The toxicity descriptors predicted that 4-dehydroxy-N-(4,5-methylenedioxy-2-nitrobenzylidene)tyramine and 2-(4-methylphenyl) ethynylaniline could exert Ames toxicity, and 4-dehydroxy-N-(4,5-methylenedioxy-2-nitrobenzylidene) tyramine could exert hepatoxicity. Oral rat acute toxicity levels expressed as the half-maximal lethal doses (LD_{50}) of the compounds, were predicted to range from 1.766 to 4.338 mol/kg.

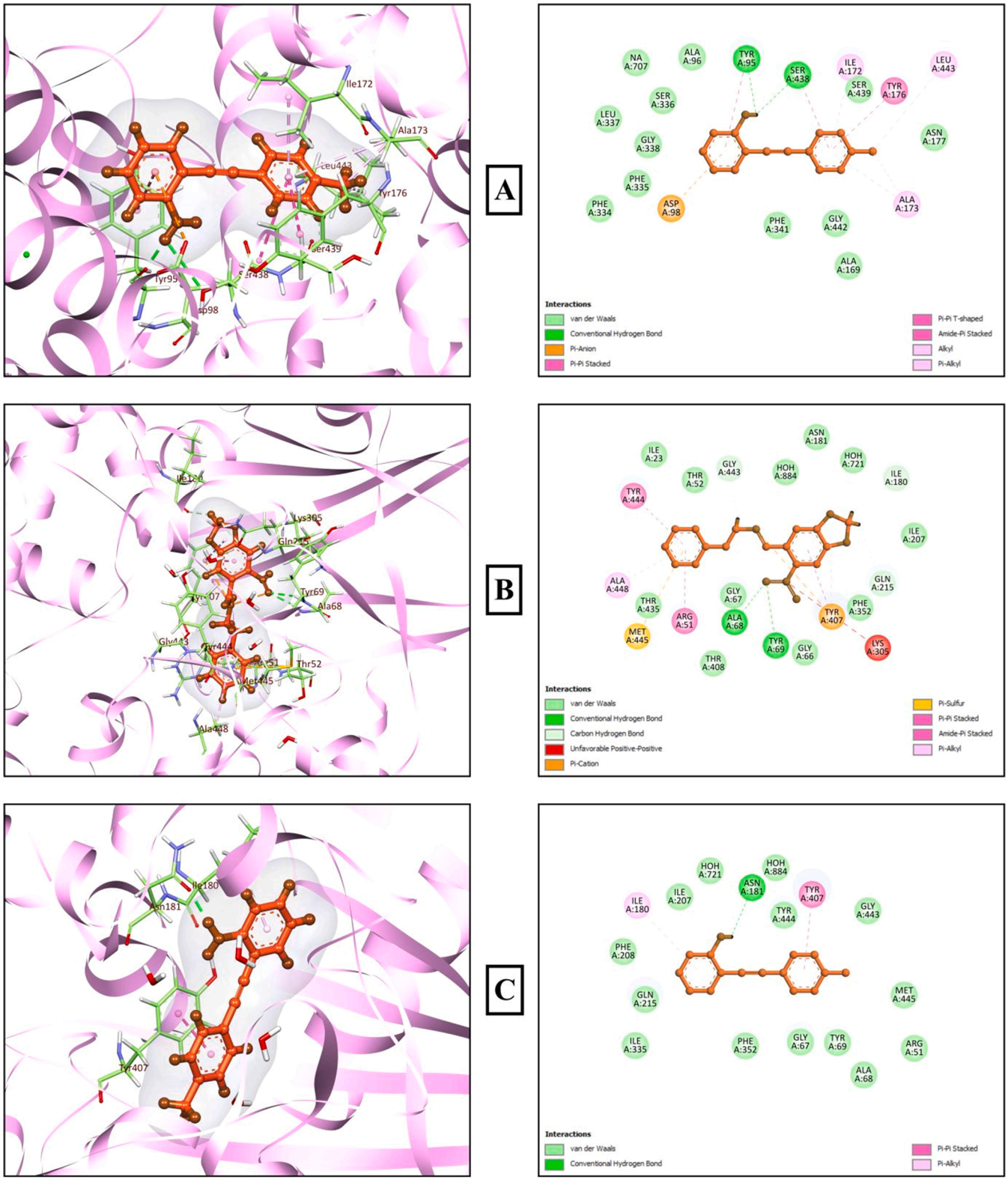

Fig. 10. Best-ranked docking poses (left) and 2D visualizations of the interactions (right) between (A) 2-(4-methylphenyl)ethynylaniline and the active site residues of SERT3 (PDB ID: 5I6X) and between (B) 4-dehydroxy-N-(4,5-methylenedioxy-2-nitrobenzylidene)tyramine and (C) 2-(4-methylphenyl)ethynylaniline and the active site residues of MAO-A (PDB ID: 2Z5Y).

4. Discussion

Plant-derived medicines have a long history of use for the prevention and treatment of human diseases [66]. The World Health Organization (WHO) stated that roughly 80% of the world's population takes herbal medicines for some form of primary health care, and much of this intervention includes the use of plant parts and their bioactive ingredients [67,68]. Herbal remedies are becoming increasingly prevalent

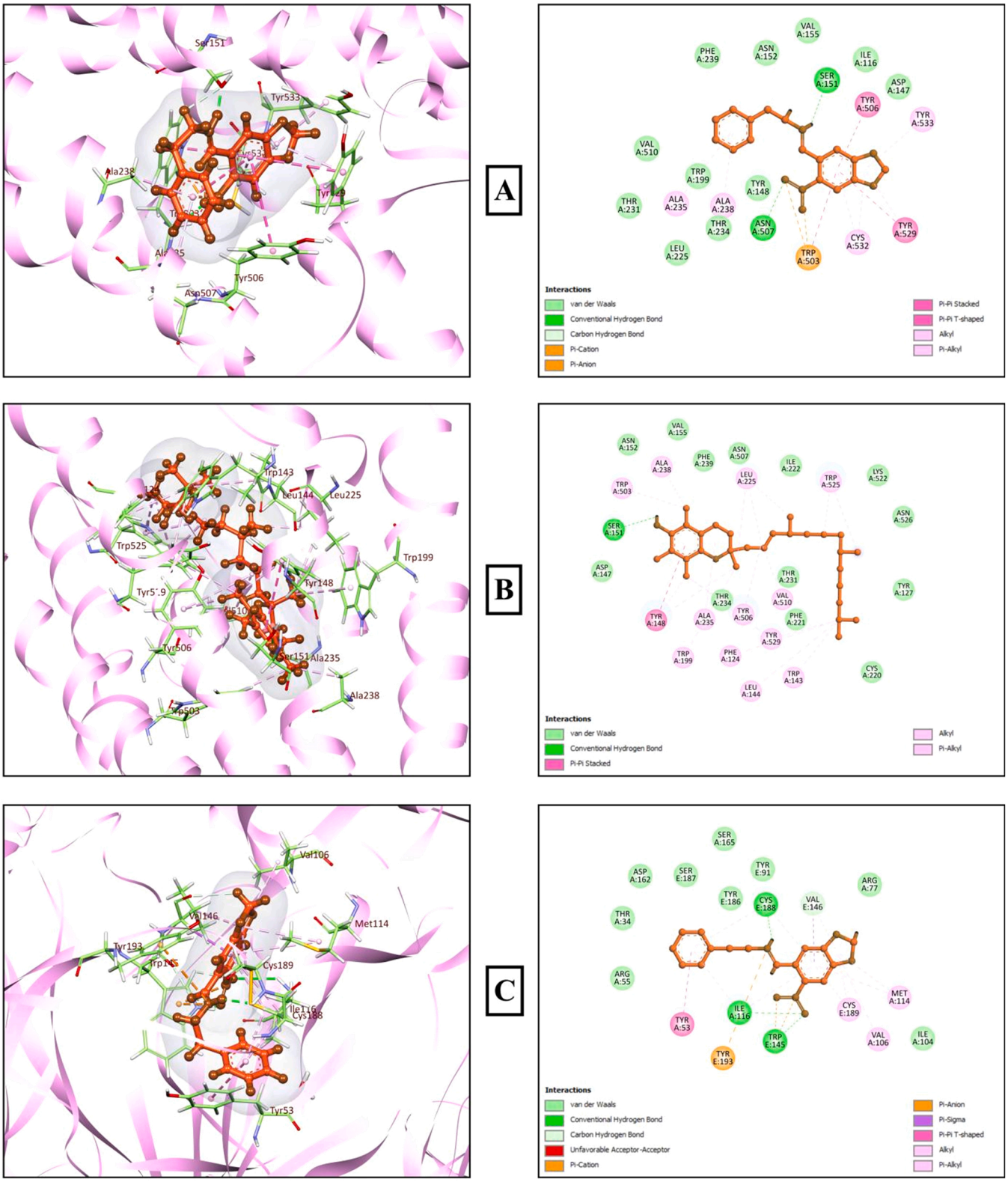

Fig. 11. Best-ranked docking poses (left) and 2D visualizations of the interaction (right) between (A) 4-dehydroxy-N-(4,5-methylenedioxy-2-nitrobenzylidene)tyramine and (B) vitamin E and the active site residues of M3MACR (PDB ID: 4U14) and between (C) 4-dehydroxy-N-(4,5-methylenedioxy-2-nitrobenzylidene)tyramine and the active site residues of the 5-HT3 receptor (PDB ID: 5AIN).

in developing countries due to the inconvenience of synthetic medicines [69]. The therapeutic value of plants is currently considered to be of significant importance due to their unique profiles as a major source of therapeutic phytocompounds that could contribute to the design of novel drugs [70,71]. In fact, numerous pharmaceutical agents that have been approved by the Food and Drug Administration (FDA) originated from plant sources [2,3,66]. In this context, the goals of this study were to (1) perform the analysis of chemical elements, moisture, ash, and

Table 5
Predicted biological activities of the major compounds from MeOH-AI by PASS online.

Compounds	Predicted Biological Activities	Pa	Pi
Alpha-Humulene	Anti-inflammatory	0.741	0.011
	Nootropic	0.634	0.062
	Transcription factor NF kappa B inhibitor	0.512	0.004
	Fibrinolytic	0.503	0.119
2TCH2H	TNF expression inhibitor	0.753	0.004
	Gastrin inhibitor	0.743	0.003
	Thrombolytic	0.734	0.002
	Antisecretoric	0.739	0.007
	Anti-inflammatory	0.701	0.016
	Cyclooxygenase 3 inhibitor	0.678	0.003
	Platelet adhesion inhibitor	0.626	0.006
	Antithrombotic	0.585	0.017
	Fibrinolytic	0.617	0.063
	Histamine release inhibitor	0.558	0.018
	Fibrinogen receptor antagonist	0.503	0.043
4DHNT	Neurotransmitter uptake inhibitor	0.739	0.007
Stigmasterol	Nootropic	0.702	0.041
	Atherosclerosis treatment	0.564	0.012
	Antinociceptive	0.601	0.008
	Anti-inflammatory	0.542	0.045
Bicyclo[8.1.0]undecane	Antineurotic	0.766	0.024
	Spasmolytic, urinary	0.713	0.009
	5-Hydroxytryptamine release stimulant	0.723	0.023
	Fibrinolytic	0.673	0.033
	Platelet adhesion inhibitor	0.624	0.007
	Neurotransmitter uptake inhibitor	0.637	0.022
	Nootropic	0.659	0.052
	Dopamine release stimulant	0.595	0.003
	Fibrinogen receptor antagonist	0.596	0.017
	Gastrin inhibitor	0.576	0.031
	Antinociceptive	0.552	0.015
	Neurodegenerative diseases treatment	0.525	0.026
	Antisecretoric	0.509	0.028
2-(4-Methylphenyl) ethynylaniline	Gastrin inhibitor	0.561	0.037
	Platelet adhesion inhibitor	0.538	0.038
Vitamin E	Anti-inflammatory	0.814	0.006
	Antianginal	0.709	0.008
	Wound healing agent	0.598	0.006
	Anti-inflammatory, ophthalmic	0.585	0.003
	Spasmolytic	0.527	0.024
	Atherosclerosis treatment	0.515	0.016
E12TD	–	–	–

Pa, Probable activity; Pi, Probable inactivity. 2TCH2H: 2,6,10,14,18,22-Tetracosahexaene, 2,6,10,15,19,23-hexamethyl-, (all-E)-; 4DHNT: 4-Dehydroxy-N-(4,5-methylenedioxy-2-nitrobenzylidene)tyramine; E12TD: Ethane, 1-(4,4,4-trifluro-1,3-dithiobutyl)− 2-(3,3,3-trifluoro-1,2-dithiopropyl)-.

organic matter content in the fresh *A. indica* whole-plant, and (2) evaluate the anti-inflammatory, thrombolytic, antidepressant, and antidiarrheal activities of a whole-plant MeOH-AI using *in vitro* assays and animal models.

TST and FST are the most frequently used animal models for testing antidepressant-like effects, and they have proven to be reliable and predictive [72]. Both of these tests are based upon the fact that when animals are subjected to short-term, unavoidable stress, they develop depressive-like behaviors that can be mitigated by antidepressant agents [63]. These two models are sensitive and quite specific to major classes of antidepressant drugs, such as tricyclics, 5-HT reuptake inhibitors, MAO inhibitors, and atypical antidepressants [73,74]. From these perspectives, in this study, we employed TST and FST to investigate the antidepressant effects of MeOH-AI. In the current study, when exposed to the stressful conditions of the TST and FST, the vehicle-treated control groups mainly displayed passive actions such as immobility behaviors, whereas the MeOH-AI treated groups exhibited increased active behaviors, such as swimming and struggling while decreasing immobility behaviors. In both tests, MeOH-AI exerted a strong antidepressant-like effect at a dose of 400 mg/kg by significantly reducing the duration of the depression-like behaviors, which was comparable to the imipramine-treated group. These findings indicate that MeOH-AI contains bioactive phytochemicals possessing promising antidepressant effects. Several plant metabolites, including flavonoids, phenolic acids, alkaloids, saponins, sapogenins, amines, carbohydrates, and terpenoids, have been reported to exert antidepressant effects via various mechanisms, such as regulation of monoamine neurotransmitter reuptake, MAO activity, neuroendocrine function, and many others [75,76]. Phytochemical constituents such as flavonoids, phenolic acids, alkaloids, terpenoids, and steroids are evidently present in *A. indica* [17,77]. It can thus be proposed that the antidepressant activity of MeOH-AI is most likely due to interactions between these phytochemicals and the neurotransmitter systems linked to depressive-like behaviors.

Various studies have been performed to confirm the antidiarrheal effects of medicinal plants by examining their biological activities, which can include antispasmodic effects, the delay of intestinal transit, the suppression of intestinal motility, the stimulation of water absorption, or the reduction in intraluminal fluid accumulation [51,55,78,79]. *A. indica* has been extensively used to treat gastric dysfunction, inflammatory disorders, and hypertension [80]. However, the current study focused on the verification of antidiarrheal activities following the administration of MeOH-AI extract to various experimental models [81,82]. The secretion of ricinoleic acid can cause the irritation and inflammation of the intestinal mucosa, associated with the release of nitric oxide, prostaglandins, and other autacoids [52,83]. Castor oil is known to alter the electrolyte permeability of the intestinal membrane, elevating prostaglandin biosynthesis and release, causing a

Table 6
Physicochemical properties of the eight potential compounds from MeOH-AI for good oral bioavailability.

Physicochemical Properties	Compounds							
	I	II	III	IV	V	VI	VII	VIII
Lipinski Rules								
MW[1]	204.35	410.72	298.29	412.69	152.28	207.27	430.71	308.35
nHBA[2]	0	0	5	1	0	0	2	6
nHBD[3]	0	0	0	1	0	1	1	0
LogP[4]	4.26	9.38	2.51	6.96	3.95	3.38	8.27	4.44
Lipinski's violations[5]	0	1	0	1	0	0	1	0
Veber Rules								
nRB[6]	0	15	5	5	0	0	12	8
TPSA[7]	0	0	76.64	20.23	0	26.02	29.46	101.2

(I) alpha-Humulene; (II) 2,6,10,14,18,22-Tetracosahexaene, 2,6,10,15,19,23-hexamethyl-, (all-E)-; (III) 4-Dehydroxy-N-(4,5-methylenedioxy-2-nitrobenzylidene) tyramine; (IV) Stigmasterol; (V): Bicyclo[8.1.0]undecane; (VI) 2-(4-Methylphenyl)ethynylaniline; (VII) Vitamin E; (VIII) Ethane, 1-(4,4,4-trifluro-1,3-dithiobutyl)− 2-(3,3,3-trifluoro-1,2-dithiopropyl)-. 1 MW, Molecular weight (acceptable range: ≤ 500). 2 nHBA, Hydrogen bond acceptor (acceptable range: ≤ 10); 3 nHBD, Hydrogen bond donor (acceptable range: ≤ 5); 4 LogP, Lipophilicity (acceptable range: ≤ 5); 5 Lipinski's violations, Number of violations of Lipinski's rule of five (acceptable range: ≤ 1); 6 nRB, Number of rotatable bonds (acceptable range: ≤ 10), 7 TPSA, Topological polar surface area (acceptable range: ≤ 140 Å2).

Table 7
Pharmacokinetics and toxicological (ADME/T) profiles of the major eight compounds from MeOH-AI.

Parameters	Compounds							
	I	II	III	IV	V	VI	VII	VIII
Absorption								
Caco2 permeability[1]	1.421	1.216	1.108	1.213	1.386	1.516	1.345	1.471
Intestinal absorption[2]	94.682	90.341	93.801	94.97	94.509	93.894	89.782	85.75
P-gp substrate	Yes	No	No	No	Yes	Yes	No	Yes
Distribution								
VDss[3]	0.505	0.411	− 0.052	0.178	0.551	0.495	0.709	− 0.058
BBB permeability[4]	0.663	0.981	− 0.515	0.771	0.711	0.584	0.876	0.653
CNS permeability[5]	− 2.555	− 0.955	− 2.222	− 1.652	− 2.46	− 1.351	− 1.669	− 2.734
Metabolism								
CYP1A2 inhibitor	No	No	Yes	No	No	Yes	No	No
CYP2C19 inhibitor	No	No	Yes	No	No	Yes	Yes	Yes
CYP2C9 inhibitor	No	No	Yes	No	No	Yes	No	No
CYP2D6 inhibitor	No	No	No	No	No	Yes	No	No
CYP3A4 inhibitor	No	No	No	No	No	No	No	No
Excretion								
Total clearance[6]	1.282	1.791	0.223	0.618	1.15	0.327	0.794	0.512
Renal OCT2 substrate	No	No	No	No	No	No	No	No
Toxicity								
Ames toxicity	No	No	Yes	No	No	Yes	No	No
Hepatotoxicity	No	No	Yes	No	No	No	No	No
Oral rat acute toxicity[7]	1.766	1.848	1.909	2.54	1.851	2.409	2.072	4.338

(I) alpha-Humulene; (II) 2,6,10,14,18,22-Tetracosahexaene, 2,6,10,15,19,23-hexamethyl-, (all-E)-; (III) 4-Dehydroxy-N-(4,5-methylenedioxy-2-nitrobenzylidene) tyramine; (IV) Stigmasterol; (V): Bicyclo[8.1.0]undecane; (VI) 2-(4-Methylphenyl)ethynylaniline; (VII) Vitamin E; (VIII) Ethane, 1-(4,4,4-trifluro-1,3-dithiobutyl)− 2-(3,3,3-trifluoro-1,2-dithiopropyl)-. 1 Caco2 permeability (expressed as log Papp in 10 −6 cm/s, (log Papp > 0.90 = high permeability); 2 Intestinal absorption (expressed in % absorbed, apsorption < 30% = poor); 3 VDss, steady state volume of distribution in human (expressed as log VDss in L/kg, log VDss < −0.15 = poor, log VDss > 0.45 = high); 4 BBB permeability (expressed as LogBB, logBB > 0.3 = high permeability, logBB <−1 = poor permeability); 5 CNS permeability (expressed as log PS, logPS > −2 = penetrable, logPS < −3 = impenetrable); 6 Total clearance (predicted total clearance log(CLtot) is given in log(mL/min/kg)); 7 Oral rat acute toxicity (expressed as LD50 in mol/kg).

pathophysiologic condition resulting in diarrhea [84,85]. The antidiarrheal activity of *A. indica* may be associated with the presence of chemical compounds that were isolated and quantified by the GC-MS analysis. The presence of zinc, potassium and other chemical elements may be responsible for diarrhea management [17,86]. These compounds are known to reduce autacoid and prostaglandin secretion [87], and the inhibition of prostaglandin E_2 is known to reduce gastrointestinal motility and the secretory response of the intestine [88].

Several natural sources, especially fruits and vegetables, have been evaluated for their components, which present anticoagulant, antiplatelet, and fibrinolytic activities, and evidence indicates that the consumption of such food can contribute to the prevention of coronary events and stroke [89–93]. The topical administration of anti-inflammatory agents at the site of inflammation is among the most effective anti-inflammatory treatments [94]. Potential anti-inflammatory efficacy is sometimes reported to be higher when an extract is administered topically compared with oral administration [95]. This phenomenon has been demonstrated for flavonoids and phenolic acids with demonstrated anti-inflammatory effects [94,96]. Flavonoids interact directly with the prostaglandin system, and various phenolic acid derivatives are thought to exert their anti-inflammatory actions through the inhibition of superoxide radical generation [24,37,97,98]. The phytochemical analysis of MeOH-AI indicated that the chemical constituents included flavonoids and phenolic acids, and the extract demonstrated good anti-inflammatory activities in the *in vitro* evaluations. Bacterial contaminants in plants express plasminogen receptors that bind plasminogen. Cell surface-bound plasminogen is freely activated into plasmin, which could regulate fibrinolysis [91]. However, some plants exert thrombolytic or fibrinolytic effects via the presence of fibrinolytic protease enzymes [66]. The bacterial plasminogen activator staphylokinase activates plasminogen to dissolve clots and disrupt the extracellular matrix and fibrin fibers that hold cells together [99,100]. The mediocre clot lysis activity observed for MeOH-AI may be due to the moderate presence of plasminogen activators, allowing cell surface-bound plasminogen to induce a minimal level of fibrinolysis.

Molecular docking is a well-established computational drug modeling approach that is widely used to delineate interactions between therapeutic molecules and target proteins (enzymes/receptors) and model potential biochemical mechanisms of action [53,101,102]. This technique is often applied to the design of drug molecules to address a wide range of complex pathologies [103]. Molecular docking aims to infer the orientation and binding strength of a drug candidate within the binding pocket of the target protein, contextualizing the potential mode of action through which naturally-originated molecules exert their biological effects and rationalizing structure-activity relationships [104]. In the current study, we integrated an *in silico* molecular docking approach to clarify the potential underlying modes of action associated with the observed anti-inflammatory, thrombolytic, antidepressant, and antidiarrheal effects of MeOH-AI and validate and correlate our experimental findings with molecular outcomes. The docking experiment conducted in this research revealed interesting insights regarding the binding of 12 major phyto-compounds identified in MeOH-AI by the GC-MS analysis and revealed several distinct target proteins known to play prominent roles in various pathological conditions, including inflammation, thrombosis, depression, and diarrhea.

When exploring the anti-inflammatory effects associated with the identified compounds, 4-dehydroxy-N-(4,5-methylenedioxy-2-nitrobenzylidene) tyramine and ethane, 1-(4,4,4-trifluro-1,3-dithiobutyl)− 2-(3,3,3-trifluoro-1,2-dithiopropyl)- demonstrated promising binding affinities for COX-2 compared with the reference drug diclofenac sodium. This observation indicated that these compounds might be able to suppress the generation of prostaglandins through COX-2 inhibition (PDB ID: 4PH9), alleviating inflammatory reactions. The molecular docking analysis performed to explore thrombolytic activity revealed that stigmasterol possessed favorable binding energies for TPA (PDB ID: 1A5H). These bioactive compounds may potentially contribute to the observed thrombolytic effects of MeOH-AI. The docking studies designed to interpret the antidepressant-like activities revealed several potential bioactive molecules that possess antidepressant effects. Among the examined compounds, 2-(4-methylphenyl) ethynylaniline demonstrated

a significantly strong binding energy against the two studied target proteins, SERT3 (PDB ID: 5I6X) and MAO-A (PDB ID: 2Z5Y), which are closely involved in the monoaminergic system. In addition, 4-dehydroxy-N-(4,5-methylenedioxy-2-nitrobenzylidene) tyramine and 2-(4-methylphenyl) ethynylaniline exerted stronger binding affinities for MAO-A than the commercially available antidepressant phenelzine. Ethane, 1-(4,4,4-trifluro-1,3-dithiobutyl)− 2-(3,3,3-trifluoro-1,2-dithiopropyl)-; and 2,6,10,14,18,22-tetracosahexaene, 2,6,10,15,19,23-hexamethyl-, (all-E)- also demonstrated encouraging binding energies for MAO-A. These docking outcomes suggest that these potential bioactive molecules found in MeOH-AI may stimulate the monoaminergic system, increasing monoamine neurotransmitter levels in the brain, including serotonin, which can attenuate depression-like behaviors. Furthermore, in an earlier docking study, 4-dehydroxy-N-(4,5-methylenedioxy-2-nitrobenzylidene) tyramine demonstrated substantial interactions with the COX-2 binding site, and COX-2 inhibitors have been reported to have both direct and indirect effects on the CNS serotonergic system, which may contribute to the observed antidepressant effects [105]. The docking analysis was performed to investigate the potential underlying biochemical pathways associated with the antidiarrheal activity observed following MeOH-AI administration, targeting two proteins known to regulate intestinal motility: M3MACR (PBD ID: 4U14) and 5-HT3 receptor (PDB ID: 5AIN). The analysis revealed that 4-dehydroxy-N-(4, 5-methylenedioxy-2-nitrobenzylidene) tyramine has a greater propensity for binding and interacting with the active residues of M3MACR and 5-HT3 receptor than the standard antidiarrheal medications (loperamide and alosetron), indicating its potential in the design of antidiarrheal therapeutics. Vitamin E also exerted significant binding effects with M3MACR. Our docking study demonstrates that these metabolites may potentially mediate the antidiarrheal effects of MeOH-AI by interacting with these target receptors.

The search for promising novel pharmacologically active candidates involves multiple factors. In addition to displaying an optimal specific activity, a drug candidate must induce minimal adverse effects alongside the targeted pharmacological attributes [106]. Therefore, to predict other relevant pharmacological properties and therapeutic targets and support the results of our experimental studies, we attempted to determine the probable biological activity spectra of the major metabolites identified in MeOH-AI via PASS online. The PASS computer algorithm enables the prediction of greater than 4000 forms of biological activity among drug-like molecules based on their structural formulas [107]. In the current analysis, the PASS program predicted several relevant pharmacological activities and potential targets for the test compounds. In addition to displaying numerous pharmacological and therapeutic potential targets, 2,6,10,14,18,22-tetracosahexaene, 2,6,10,15,19,23-hexamethyl- was estimated to act as potent inhibitors of TNF expression and gastrin, and the Pa values for thrombolytic, antisecretory, and anti-inflammatory activities were greater than 0.7. Vitamin E, stigmasterol, and α-humulene were also estimated to display a range of probable pharmacological activities with encouraging Pa values, which were consistent with our experimental investigation. Vitamin E has previously been demonstrated to induce anti-inflammatory, neuroprotective, and cholesterol-reducing effects [108], in addition to the minimization of platelet hyper-aggregation, which can contribute to atherosclerosis. Vitamin E also tends to decrease prostaglandin synthesis, which can trigger platelet clumping [109]. Stigmasterol has been demonstrated to possess anti-inflammatory and neuroprotective properties [110]. These findings suggest that the predicted pharmacological and therapeutic properties of the test compounds aligned with our experimental findings. Therefore, the recorded pharmacological activities of MeOH-AI are likely attributable to the synergistic effects of its bioactive metabolites, both those explored in the current study and potentially other metabolites that have yet to be characterized.

Over the past few decades, a staggeringly high clinical trial failure rate has resulted in the emergence of only a few new drugs from among hundreds of candidates [111]. The key factors that prevent nearly half of all tested therapeutic agents from entering the market include pharmacokinetic and toxicity complications [112]. The ADME/T parameters of a given compound are considered to be the key determinants of clinical efficacy, regardless of the potential pharmacological characteristics [113]. We, therefore, scrutinized the eight best-ranked compounds from the molecular docking and PASS analyses for their ADME/T profiles via SwissADME and pkCSM *in silico* ADME/T descriptor tools. The oral bioavailability qualities of the compounds were characterized according to the physicochemical parameters imposed by Lipinski's RoF and Veber's rules. Among pharmacokinetic properties, poor or highly inconsistent oral bioavailability are critical factors that can prevent drug development [114]. Lipinski's RoF states that molecules are likely to possess optimum aqueous solubility and intestinal permeability if they meet at least three of the following four physicochemical criteria: molecular weight ≤ 500, number of H-bond acceptors ≤ 10, number of H-bond donors ≤ 5, and partition coefficient (logP) ≤ 5 [115]. Veber et al. [116] believed that compounds containing 10 or fewer rotatable bonds and 140 $Å^2$ or less topological polar surface area (TPSA) would be more likely to display good oral bioavailability. Our *in silico* analysis revealed that the physicochemical characteristics of the studied compounds aligned well with most of Lipinski's and Veber's rules, indicating favorable absorption or permeation outcomes. The complexity of the BBB can prevent therapeutic agents from accessing the brain and limiting CNS exposure, preventing therapeutic efficacy for some disorders [117]. The potential ability for a drug to cross the BBB is essential for the treatment of CNS disorders [118]. In the current ADME/T evaluation, the distribution descriptors predicted efficient BBB and CNS permeability for most of the compounds, in addition to desirable VDss values, suggesting good bioavailability. The inhibition of CYP, which is the primary mechanism for drug metabolism, typically requires competition with another drug for the same enzyme binding site. The inhibition of CYP disrupts the biotransformation and clearance of all clinically used medications and can contribute to toxicity or loss of efficacy [119]. In this research, the metabolic profiles for half of the tested compounds were non-inhibitors of all CYP enzymes, whereas one-fourth of the compounds were predicted to inhibit CYP2C19 only. Except for 2-(4-methylphenyl)ethylaniline, all compounds were presumed not to suppress CYP2D6 functions, which is a determinant in biotransformation pathways [119]. The prediction of excretion parameters revealed that the total clearance of 2,6,10,14,18,22-tetracosahexaene, 2,6,10,15,19,23-hexamethyl-, (all-E)- is the highest, followed by α-humulene, and bicyclo [8.1.0] undecane. All of the tested compounds were estimated to possess low toxic potential. This research provides a deeper understanding of the pharmacological pathways through which MeOH-AI and its bioactive metabolites mediate various activities through the examination of experimental and computer-assisted models.

5. Conclusions

The MeOH-AI displayed analgesic effects in both central and peripheral pain models. Besides, it has shown antidepressants and anxiolytic behavior with lower sedative side effects in the present neuropharmacological research. The observed bioactive effects were significant and dose-dependent. The results of elemental analysis and organic matter content indicated the presence of a variety of essential elements and probabilistic bioactive organic compounds that may affect a variety of diseases, such as diarrhea. Computer-aided analyses and molecular docking indicated potential neuropharmacological affinities, including antidepressant activity through binding with SERT3, antidiarrheal activity through binding with M3MACR, and anti-inflammatory activity through binding with COX-2. Further studies must be performed to determine the dose-response analysis and clarify the neuropharmacology and antidiarrheal effects of possible compounds in the animal model.

Ethical approval

The Planning and Development (P & D) Committee of the Department of Pharmacy, International Islamic University Chittagong, Bangladesh, approved the animal handling procedures (Pharm-P&D-138/13-'19).

Funding

This research did not receive any specific grant from funding agencies in the public, commercial, or not-for-profit sectors.

CRediT authorship contribution statement

Suaad Nasrin: Conceptualization, Methodology, Investigation, Data curation, Software, Formal analysis, Writing – original draft. **Mohammad Nazmul Islam:** Methodology, Data curation, Formal analysis, Writing – original draft, Writing – review & editing. **Mohammed Abu Tayab:** Methodology, Validation, Visualization, Writing – review & editing. **Mst. Samima Nasrin:** Methodology, Validation, Visualization. **Md. Abu Bakar Siddique:** Methodology, Investigation, Data curation, Formal analysis, Validation, Visualization, Writing – review & editing. **Talha Bin Emran:** Funding acquisition, Resources, Project administration, Writing – review & editing, Supervision. **A. S. M. Ali Reza:** Funding acquisition, Resources, Project administration, Writing – review & editing, Supervision.

Conflict of interest statement

The authors declare that they have no known competing financial interests or personal relationships that could have appeared to influence the work reported in this paper.

Data Availability

The datasets supporting the conclusions of this study are included in the article.

Acknowledgments

The authors are very much thankful to the Department of Pharmacy, International Islamic University Chittagong, Bangladesh; and Bangladesh Council of Scientific and Industrial Research (BCSIR), Dhaka, Bangladesh for the laboratory, and other vital logistic support for this research. The authors would like to thank Cambridge Proofreading & Editing LLC. (https://proofreading.org/) for editing a draft of this manuscript.

Appendix A. Supporting information

Supplementary data associated with this article can be found in the online version at doi:10.1016/j.biopha.2022.112842.

References

[1] A. Ghasemzadeh, H.Z.E. Jaafar, A. Rahmat, Optimization protocol for the extraction of 6-gingerol and 6-shogaol from Zingiber officinale var. rubrum Theilade and improving antioxidant and anticancer activity using response surface methodology, BMC Complement. Altern. Med. 15 (1) (2015) 258.
[2] M. Rahman, M. Uddin, A. Reza, A.M. Tareq, T.B. Emran, J. Simal-Gandara, Ethnomedicinal value of antidiabetic plants in bangladesh: a comprehensive review, Plants 10 (4) (2021) 729.
[3] M.M. Rahman, A.M.A. Reza, M.A. Khan, K.M. Sujon, R. Sharmin, M. Rashid, M. G. Sadik, M.A. Reza, T. Tsukahara, R. Capasso, Unfolding the apoptotic mechanism of antioxidant enriched-leaves of tabebuia pallida (Lindl.) miers in EAC cells and mouse model, J. Ethnopharmacol. (2021), 114297.
[4] K.H. Hossain, M.A. Rahman, M. Taher, J. Tangpong, D. Hajjar, W. Alelwani, A. A. Makki, A.A. Reza, Hot Methanol Extract of Leea Macrophylla (Roxb.) manages chemical-induced inflammation in Rodent Model, J. King Saud. Univ. -Sci. (2020).
[5] A.S.M. Ali Reza, M.S. Nasrin, M.A. Hossen, M.A. Rahman, I. Jantan, M.A. Haque, E. Sobarzo-Sánchez, Mechanistic insight into immunomodulatory effects of food-functioned plant secondary metabolites, Crit. Rev. Food Sci. Nutr. (2021) 1–31.
[6] M.A. Hoque, S. Ahmad, N. Chakrabarty, M.F. Khan, M.S.H. Kabir, A. Brishti, M. O. Raihan, A.K. Alam, M.A. Haque, M.S. Nasrin, Antioxidative role of palm grass rhizome ameliorates anxiety and depression in experimental rodents and computer-aided model, Heliyon 7 (10) (2021), e08199.
[7] A.A. Reza, M.A. Haque, J. Sarker, M.S. Nasrin, M.M. Rahman, A.M. Tareq, Z. Khan, M. Rashid, M.G. Sadik, T. Tsukahara, Antiproliferative and antioxidant potentials of bioactive edible vegetable fraction of Achyranthes ferruginea Roxb. in cancer cell line, Food Sci. Nutr. (2021).
[8] M. Kao, Popular herbal remedies of Taiwan, Southern Materials Center Publishing Inc, Taipei, 1985, p. 89.
[9] M.A. Rahman, S. Uddin, C. Wilcock, Medicinal plants used by Chakma tribe in Hill Tracts districts of Bangladesh, (2007).
[10] M. Yusuf, J. Chowdhury, M. Wahab, J. Begum, Medicinal plants of Bangladesh, Bangladesh Council of Scientific and Industrial Research,, Dhaka, Bangladesh, 1994.
[11] M. Uddin, A. Ali Reza, M. Abdullah-Al-Mamun, M.S. Kabir, M. Nasrin, S. Akhter, M. Arman, S. Islam, M. Rahman, Antinociceptive and anxiolytic and sedative effects of methanol extract of anisomeles indica: an experimental assessment in mice and computer aided models, Front. Pharmacol. 9 (2018) 246.
[12] K. Fern, Tropical plants database. tropical. theferns. info, Retrieved from tropi cal. thefe rns. info/viewt ropic al. php, 2018.
[13] A. Sundriyal, K.R.V. Bijjem, A.N. Kalia, Antiepileptic potential of Anisomeles indica (Linn.) Kuntze aerial parts in pentylenetetrazole-induced experimental convulsions in Wistar rats, (2013).
[14] M. Dharmasiri, W. Ratnasooriya, M. Thabrew, Anti-inflammatory activity of decoctions of leaves and stems of Anisomeles indica at preflowering and flowering stages, Pharm. Biol. 40 (6) (2002) 433–439.
[15] Y.C. Wang, T.L. Huang, Screening of anti-Helicobacter pylori herbs deriving from Taiwanese folk medicinal plants, Pathog. Dis. 43 (2) (2005) 295–300.
[16] S.-C. Hsieh, S.-H. Fang, Y.K. Rao, Y.-M. Tzeng, Inhibition of pro-inflammatory mediators and tumor cell proliferation by Anisomeles indica extracts, J. Ethnopharmacol. 118 (1) (2008) 65–70.
[17] Y.K. Rao, S.-H. Fang, S.-C. Hsieh, T.-H. Yeh, Y.-M. Tzeng, The constituents of Anisomeles indica and their anti-inflammatory activities, J. Ethnopharmacol. 121 (2) (2009) 292–296.
[18] H.-C. Huang, H.-M. Lien, H.-J. Ke, L.-L. Chang, C.-C. Chen, T.-M. Chang, Antioxidative characteristics of Anisomeles indica extract and inhibitory effect of ovatodiolide on melanogenesis, Int. J. Mol. Sci. 13 (5) (2012) 6220–6235.
[19] M. Dharmasiri, W. Ratnasooriya, M.I. Thabrew, Water extract of leaves and stems of preflowering but not flowering plants of Anisomeles indica possesses analgesic and antihyperalgesic activities in rats, Pharm. Biol. 41 (1) (2003) 37–44.
[20] Y.-C. Wang, T.-L. Huang, Screening of anti-Helicobacter pylori herbs deriving from Taiwanese folk medicinal plants, FEMS Immunol. Med. Microbiol. 43 (2) (2005) 295–300.
[21] M.J. Uddin, M. Abdullah-Al-Mamun, K. Biswas, M. Asaduzzaman, M.M. Rahman, Assessment of anticholinesterase activities and antioxidant potentials of Anisomeles indica relevant to the treatment of Alzheimer's disease, Orient. Pharm. Exp. Med. 16 (2) (2016) 113–121.
[22] O. Berton, E.J. Nestler, New approaches to antidepressant drug discovery: beyond monoamines, Nat. Rev. Neurosci. 7 (2) (2006) 137–151.
[23] C. Han, C.-U. Pae, Pain and depression: a neurobiological perspective of their relationship, Psychiatry Investig. 12 (1) (2015) 1.
[24] J.N.R. Moni, M. Adnan, A.M. Tareq, M. Kabir, A. Reza, M. Nasrin, K. H. Chowdhury, S.A.J. Sayem, M.A. Rahman, A. Alam, Therapeutic potentials of syzygium fruticosum fruit (Seed) reflect into an array of pharmacological assays and prospective receptors-mediated pathways, Life 11 (2) (2021) 155.
[25] L.E. Schechter, R.H. Ring, C.E. Beyer, Z.A. Hughes, X. Khawaja, J.E. Malberg, S. Rosenzweig-Lipson, Innovative approaches for the development of antidepressant drugs: current and future strategies, NeuroRx 2 (4) (2005) 590–611.
[26] D. Sivaraman, G. Vignesh, R. Selvaraj, B. Dare, Identification of potential monoamine oxidase inhibitor from herbal source for the treatment of major depressive disorder: an in-silico screening approach, Der. Pharma Chem. 7 (2015) 224–234.
[27] A.M. Tareq, S. Farhad, A.N. Uddin, M. Hoque, M.S. Nasrin, M.M.R. Uddin, M. Hasan, A. Sultana, M.S. Munira, C. Lyzu, Chemical profiles, pharmacological properties, and in silico studies provide new insights on Cycas pectinata, Heliyon 6 (6) (2020), e04061.
[28] S.M. Stahl, J.F. Pradko, B.R. Haight, J.G. Modell, C.B. Rockett, S. Learned-Coughlin, A review of the neuropharmacology of bupropion, a dual norepinephrine and dopamine reuptake inhibitor, Prim. Care Companion J. Clin. Psychiatry 6 (4) (2004) 159.
[29] E. Eriksson, Antidepressant drugs: does it matter if they inhibit the reuptake of noradrenaline or serotonin? Acta Psychiatr. Scand. 101 (2000) 12–17.
[30] E. Penn, D.K. Tracy, The drugs don't work? Antidepressants and the current and future pharmacological management of depression, Ther. Adv. Psychopharmacol. 2 (5) (2012) 179–188.
[31] P. Mantri, D.T. Witiak, Inhibitors of cyclooxygenase and 5-lipoxygenase, Curr. Med. Chem. 1 (4) (1994) 328.

[32] S. Beg, S. Swain, H. Hasan, M.A. Barkat, M.S. Hussain, Systematic review of herbals as potential anti-inflammatory agents: Recent advances, current clinical status and future perspectives, Pharmacogn. Rev. 5 (10) (2011) 120.
[33] C.N. Serhan, J. Savill, Resolution of inflammation: the beginning programs the end, Nat. Immunol. 6 (12) (2005) 1191–1197.
[34] M.S. Hossain, A.A. Reza, M.M. Rahaman, M.S. Nasrin, M.R.U. Rahat, M.R. Islam, M.J. Uddin, M.A. Rahman, Evaluation of morning glory (Jacquemontia tamnifolia (L.) Griseb) leaves for antioxidant, antinociceptive, anticoagulant and cytotoxic activities, J. Basic Clin. Physiol. Pharmacol. 29 (3) (2018) 291–299.
[35] D.M. Mosser, J.P. Edwards, Exploring the full spectrum of macrophage activation, Nat. Rev. Immunol. 8 (12) (2008) 958–969.
[36] S.A. Sakib, A.M. Tareq, A. Islam, A. Rakib, M.N. Islam, M.A. Uddin, M. Rahman, V. Seidel, T.B. Emran, Anti-inflammatory, thrombolytic and hair-growth promoting activity of the n-hexane fraction of the methanol extract of Leea indica leaves, Plants 10 (6) (2021) 1081.
[37] Y.-T. Lee, M.-J. Don, C.-H. Liao, H.-W. Chiou, C.-F. Chen, L.-K. Ho, Effects of phenolic acid esters and amides on stimulus-induced reactive oxygen species production in human neutrophils, Clin. Chim. Acta 352 (1–2) (2005) 135–141.
[38] W.T. Tadesse, A.E. Hailu, A.E. Gurmu, A.F. Mechesso, Experimental assessment of antidiarrheal and antisecretory activity of 80% methanolic leaf extract of Zehneria scabra in mice, BMC Complement. Altern. Med. 14 (1) (2014) 1–8.
[39] S. Ahmad, M.S. Nasrin, A.A. Reza, N. Chakrabarty, M.A. Hoque, S. Islam, M. S. Hafez Kabir, S.M. Tareq, A.K. Alam, M.A. Haque, Curculigo recurvata WT Aiton exhibits anti-nociceptive and anti-diarrheal effects in Albino mice and an in silico model, Anim. Models Exp. Med. 3 (2) (2020) 169–181.
[40] R.I. Glass, J.F. Lew, R.E. Gangarosa, C.W. LeBaron, M.-S. Ho, Estimates of morbidity and mortality rates for diarrheal diseases in American children, The, J. Pediatr. 118 (4) (1991) S27–S33.
[41] A.K. Das, S.C. Mandal, S.K. Banerjee, S. Sinha, J. Das, B. Saha, M. Pal, Studies on antidiarrhoeal activity of Punica granatum seed extract in rats, J. Ethnopharmacol. 68(1-3) (1999) 205–208.
[42] A. Degu, E. Engidawork, W. Shibeshi, Evaluation of the anti-diarrheal activity of the leaf extract of Croton macrostachyus Hocsht. ex Del.(Euphorbiaceae) in mice model, BMC Complement. Altern. Med. 16 (1) (2016) 1–11.
[43] T. Sarkar, M. Salauddin, S. Pati, H.I. Sheikh, R. Chakraborty, Application of raw and differently dried Pineapple (Ananas comosus) pulp on Rasgulla (sweetened Casein Ball) to enhance its phenolic profile, shelf life, and in-vitro digestibility characteristics, J. Food Process. Preserv. 45 (3) (2021), e15233.
[44] A.B. Hasan, A.S. Reza, S. Kabir, M.A.B. Siddique, M.A. Ahsan, M.A. Akbor, Accumulation and distribution of heavy metals in soil and food crops around the ship breaking area in southern Bangladesh and associated health risk assessment, SN Appl. Sci. 2 (2) (2020) 1–18.
[45] M.A.B. Siddique, M.K. Alam, S. Islam, M.T.M. Diganta, M.A. Akbor, U.H. Bithi, A. I. Chowdhury, A.A. Ullah, Apportionment of some chemical elements in soils around the coal mining area in northern Bangladesh and associated health risk assessment, Environ. Nanotechnol., Monit. Manag. 14 (2020), 100366.
[46] M.A. Ahsan, F. Satter, M.A.B. Siddique, M.A. Akbor, S. Ahmed, M. Shajahan, R. Khan, Chemical and physicochemical characterization of effluents from the tanning and textile industries in Bangladesh with multivariate statistical approach, Environ. Monit. Assess. 191 (9) (2019) 1–24.
[47] T.N. OECD, 423: Acute Oral Toxicity–OECD Guideline for the Testing of Chemical s Section 4, OECD Publishing, 2002.
[48] H. Hossain, Evaluation of antinociceptive and antioxidant activities of whole plant extract of Bacopa monniera, Res. J. Med. Plant 6 (8) (2012) 607–614.
[49] A. Hossen, M. Arman, S.A.J. Sayem, M.R.A. Maruf, M. Ahsan, M.N.I. Ullah, N. Banu, N. Alam, S.A. Sakib, Qualitative phytochemicals and pharmacological properties analysis of methanol extract of Tabernaemontana pauciflora leaves.
[50] M. Taufiq-Ur-Rahman, J.A. Shilpi, M. Ahmed, C.F. Hossain, Preliminary pharmacological studies on Piper chaba stem bark, J. Ethnopharmacol. 99 (2) (2005) 203–209.
[51] S. Bellah, M. Islam, M. Karim, M. Rahaman, M. Nasrin, M. Rahman, A. Reza, Evaluation of cytotoxic, analgesic, antidiarrheal and phytochemical properties of Hygrophila spinosa (T. Anders) whole plant, J. Basic Clin. Physiol. Pharmacol. 28 (2) (2017) 185–190.
[52] N. Mascolo, A.A. Izzo, G. Autore, F. Barbato, F. Capasso, Nitric oxide and castor oil-induced diarrhea, J. Pharmacol. Exp. Ther. 268 (1) (1994) 291–295.
[53] N. Banu, N. Alam, M. Nazmul Islam, S. Islam, S.A. Sakib, N.B. Hanif, M. Chowdhury, A.M. Tareq, K. Hasan Chowdhury, S. Jahan, Insightful valorization of the biological activities of pani heloch leaves through experimental and computer-aided mechanisms, Molecules 25 (21) (2020) 5153.
[54] A. Gokhale, V. Dikshit, A. Damre, K. Kulkarni, M. Saraf, Influence of ethanolic extract of Tephrosia purpurea Linn. on mast cells and erythrocytes membrane integrity, (2000).
[55] S. Alam, N.U. Emon, S. Shahriar, F.T. Richi, M.R. Haque, M.N. Islam, S.A. Sakib, A. Ganguly, Pharmacological and computer-aided studies provide new insights into Millettia peguensis Ali (Fabaceae), Saudi Pharmaceutical Journal, 2020.
[56] J.C. Shelley, A. Cholleti, L.L. Frye, J.R. Greenwood, M.R. Timlin, M. Uchimaya, Epik: a software program for pK a prediction and protonation state generation for drug-like molecules, J. Comput. Aided Mol. Des. 21 (12) (2007) 681–691.
[57] B.J. Orlando, M.J. Lucido, M.G. Malkowski, The structure of ibuprofen bound to cyclooxygenase-2, J. Struct. Biol. 189 (1) (2015) 62–66.
[58] M. Renatus, W. Bode, R. Huber, J. Stürzebecher, D. Prasa, S. Fischer, U. Kohnert, M.T.J.J.o.B.C. Stubbs, Structural mapping of the active site specificity determinants of human tissue-type plasminogen activator: implications for the design of low molecular weight substrates and inhibitors, 272(35) (1997) 21713–21719.
[59] J.A. Coleman, E.M. Green, E. Gouaux, X-ray structures and mechanism of the human serotonin transporter, Nature 532 (7599) (2016) 334–339.
[60] S.Y. Son, J. Ma, Y. Kondou, M. Yoshimura, E. Yamashita, T. Tsukihara, Structure of human monoamine oxidase A at 2.2-Å resolution: The control of opening the entry for substrates/inhibitors, Proc. Natl. Acad. Sci. USA 105 (15) (2008) 5739–5744.
[61] T.S. Thorsen, R. Matt, W.I. Weis, B.K.J.S. Kobilka, Modified T4 lysozyme fusion proteins facilitate G protein-coupled receptor crystallogenesis, Structure 22 (11) (2014) 1657–1664.
[62] K.L. Price, R.K. Lillestol, C. Ulens, S.C.R. Lummis, Varenicline interactions at the 5-HT3 receptor ligand binding site are revealed by 5-HTBP, ACS Chem. Neuroscience 6 (7) (2015) 1151–1157.
[63] M.A. Tayab, K.A.A. Chowdhury, M. Jabed, S. Mohammed Tareq, A.T.M.M. Kamal, M.N. Islam, A.M.K. Uddin, M.A. Hossain, T.B. Emran, J. Simal-Gandara, Antioxidant-rich woodfordia fruticosa leaf extract alleviates depressive-like behaviors and impede hyperglycemia, Plants 10 (2) (2021) 287.
[64] R.A. Friesner, J.L. Banks, R.B. Murphy, T.A. Halgren, J.J. Klicic, D.T. Mainz, M. P. Repasky, E.H. Knoll, M. Shelley, J.K. Perry, D.E. Shaw, P. Francis, P.S. Shenkin, Glide: a new approach for rapid, accurate docking and scoring. 1. method and assessment of docking accuracy, J. Med. Chem. 47 (7) (2004) 1739–1749.
[65] M.P. Repasky, M. Shelley, R.A. Friesner, Flexible Ligand Docking with Glide, John Wiley & Sons, Inc, 2007.
[66] T.B. Emran, M.A. Rahman, M.M.N. Uddin, M.M. Rahman, M.Z. Uddin, R. Dash, C. Layzu, Effects of organic extracts and their different fractions of five Bangladeshi plants on in vitro thrombolysis, BMC Complement. Altern. Med. 15 (1) (2015) 128.
[67] D. Krishnaiah, R. Sarbatly, R. Nithyanandam, A review of the antioxidant potential of medicinal plant species, Food Bioprod. Process. 89 (3) (2011) 217–233.
[68] T. Sen, S.K. Samanta, Medicinal plants, human health and biodiversity: a broad review, in: J. Mukherjee (Ed.), Biotechnological Applications of Biodiversity, Springer Berlin Heidelberg, Berlin, Heidelberg, 2015, pp. 59–110.
[69] R. Capasso, A.A. Izzo, L. Pinto, T. Bifulco, C. Vitobello, N. Mascolo, Phytotherapy and quality of herbal medicines, in: Fitoterapia, 71, 2000, pp. S58–S65.
[70] N.J.M.A.P. Azwanida, A review on the extraction methods use in medicinal plants, principle, strength and limitation, 4(196) (2015) 2167–0412.
[71] M.S. Islam, M.M. Rashid, A.A. Ahmed, A.A. Reza, M.A. Rahman, T.R. Choudhury, The food ingredients of different extracts of Lasia spinosa (L.) Thwaites can turn it into a potential medicinal food, NFS J. 25 (2021) 56–69.
[72] A.-M. Yao, F.-F. Ma, L.-L. Zhang, F. Feng, Effect of aqueous extract and fractions of Zhi-Zi-Hou-Pu decoction against depression in inescapable stressed mice: Restoration of monoamine neurotransmitters in discrete brain regions, Pharm. Biol. 51 (2) (2013) 213–220.
[73] F. Subhan, N. Karim, A.H. Gilani, R.D.E. Sewell, Terpenoid content of Valeriana wallichii extracts and antidepressant-like response profiles, Phytother. Res. 24 (5) (2010) 686–691.
[74] Y.-H. Shen, Y. Zhou, C. Zhang, R.-H. Liu, J. Su, X.-H. Liu, W.-D. Zhang, Antidepressant effects of methanol extract and fractions of Bacopa monnieri, Pharm. Biol. 47 (4) (2009) 340–343.
[75] R. Bahramsoltani, M.H. Farzaei, M.S. Farahani, R. Rahimi, Phytochemical constituents as future antidepressants: a comprehensive review %, J. Rev. Neurosci. 26 (6) (2015) 699–719.
[76] G. Lee, H. Bae, Therapeutic effects of phytochemicals and medicinal herbs on depression, BioMed. Res. Int. 2017 (2017), 6596241.
[77] G. Basappa, V. Kumar, B.K. Sarojini, D.V. Poornima, H. Gajula, T. K. Sannabommaji, J. Rajashekar, Chemical composition, biological properties of Anisomeles indica Kuntze essential oil, Ind. Crops Prod. 77 (2015) 89–96.
[78] S. Pérez-Gutiérrez, D. Zavala-Mendoza, A. Hernández-Munive, Á. Mendoza-Martínez, C. Pérez-González, E. Sánchez-Mendoza, Antidiarrheal activity of 19-deoxyicetexone isolated from Salvia ballotiflora Benth in mice and rats, Molecules 18 (8) (2013) 8895–8905.
[79] P. Ansari, M.J. Uddin, M.M. Rahman, M. Abdullah-Al-Mamun, M.R. Islam, M. H. Ali, A.A. Reza, Anti-inflammatory, anti-diarrheal, thrombolytic and cytotoxic activities of an ornamental medicinal plant: persicaria orientalis, J. Basic Clin. Physiol. Pharmacol. 28 (1) (2017) 51–58.
[80] V.K. Baranwal, R. Irchhaiya, S. Singh, Anisomeles indica: an overview, Int. Res. J. Pharm. 3 (2012) 84–87.
[81] W.T. Tadesse, A.E. Hailu, A.E. Gurmu, A.F. Mechesso, Experimental assessment of antidiarrheal and antisecretory activity of 80% methanolic leaf extract of Zehneria scabra in mice, BMC Complement. Altern. Med. 14 (1) (2014) 460.
[82] M.A. Hossen, A. Ali Reza, M.B. Amin, M.S. Nasrin, T.A. Khan, M.H.R. Rajib, A.M. Tareq, M.A. Haque, M.A. Rahman, M.A. Haque, Bioactive metabolites of Blumea lacera attenuate anxiety and depression in rodents and computer-aided model, Food Science & Nutrition.
[83] N.F. Pierce, C.C. Carpenter, H.L. Elliott, W.B. Greenough, Effects of prostaglandins, theophylline, and cholera exotoxin upon transmucosal water and electrolyte movement in the canine jejunum, Gastroenterology 60 (1) (1971) 22–32.
[84] S. Besra, A. Gomes, L. Chaudhury, J. Vedasiromoni, D. Ganguly, Antidiarrhoeal activity of seed extract of Albizzia lebbeck Benth, Phytother. Res. Int. J. Devoted Pharmacol. Toxicol. Eval. Nat. Prod. Deriv. 16 (6) (2002) 529–533.
[85] S. Brijesh, P. Daswani, P. Tetali, N. Antia, T. Birdi, Studies on the antidiarrhoeal activity of Aegle marmelos unripe fruit: Validating its traditional usage, BMC Complement. Altern. Med. 9 (1) (2009) 47.

[86] J.M. Barbosa Filho, Md.F. Agra, G. Thomas, Botanical, chemical and pharmacological investigation on Cissampelos species from Paraíba (Brazil), Ciênc. Cult. 49 (5/6) (1997) 386–394.
[87] L.-H.F.S. de Medina, J. Gálvez, M. González, A. Zarzuelo, K.E. Barrett, Effects of quercetin on epithelial chloride secretion, Life Sci. 61 (20) (1997) 2049–2055.
[88] B. Ramakrishna, M. Mathan, V. Mathan, Alteration of colonic absorption by long-chain unsaturated fatty acids: influence of hydroxylation and degree of unsaturation, Scand. J. Gastroenterol. 29 (1) (1994) 54–58.
[89] C. Torres-Urrutia, L. Guzman, G. Schmeda-Hirschmann, R. Moore-Carrasco, M. Alarcon, L. Astudillo, M. Gutierrez, G. Carrasco, J.A. Yuri, E. Aranda, Antiplatelet, anticoagulant, and fibrinolytic activity in vitro of extracts from selected fruits and vegetables, Blood Coagul. Fibrinolysis 22 (3) (2011) 197–205.
[90] L.A. Bazzano, J. He, L.G. Ogden, C.M. Loria, S. Vupputuri, L. Myers, P.K. Whelton, Fruit and vegetable intake and risk of cardiovascular disease in US adults: the first National Health and Nutrition Examination Survey Epidemiologic Follow-up Study, Am. J. Clin. Nutr. 76 (1) (2002) 93–99.
[91] M. Verstraete, Third-generation thrombolytic drugs, Am. J. Med. 109 (1) (2000) 52–58.
[92] A.A. Reza, M.S. Hossain, S. Akhter, M.R. Rahman, M.S. Nasrin, M.J. Uddin, G. Sadik, A.K. Alam, In vitro antioxidant and cholinesterase inhibitory activities of Elatostema papillosum leaves and correlation with their phytochemical profiles: a study relevant to the treatment of Alzheimer's disease, BMC Complement. Altern. Med. 18 (1) (2018) 123.
[93] O. Bahattab, I. Khan, S. Bawazeer, A. Rauf, M.N. Qureshi, Y.S. Al-Awthan, N. Muhammad, A. Khan, M. Akram, M.N. Islam, Synthesis and biological activities of alcohol extract of black cumin seeds (Bunium persicum)-based gold nanoparticles and their catalytic applications, Green Process. Synth 10 (1) (2021) 440–455.
[94] R. Casado, A. Landa, J. Calvo, J.M. Garcia-Mina, A. Marston, K. Hostettmann, M. I. Calvo, Anti-inflammatory, antioxidant and antifungal activity of Chuquiraga spinosa, Pharm. Biol. 49 (6) (2011) 620–626.
[95] M. del Carmen Recio, R.M. Giner, S. Manez, J.L. Ríos, Structural considerations on the iridoids as anti-inflammatory agents, Planta Med. 60 (03) (1994) 232–234.
[96] M.A. Hossen, A.A. Reza, A.A. Ahmed, M.K. Islam, I. Jahan, R. Hossain, M.F. Khan, M.R.A. Maruf, M.A. Haque, M.A. Rahman, Pretreatment of Blumea lacera leaves ameliorate acute ulcer and oxidative stress in ethanol-induced Long-Evan rat: a combined experimental and chemico-biological interaction, Biomed. Pharmacother. 135 (2021), 111211.
[97] A. Panthong, W. Tassaneeyakul, D. Kanjanapothi, P. Tantiwachwuttikul, V. Reutrakul, Anti-inflammatory activity of 5, 7-dimethoxyflavone, Planta Med. 55 (02) (1989) 133–136.
[98] M.N. Islam, A. Rauf, F.I. Fahad, T.B. Emran, S. Mitra, A. Olatunde, M.A. Shariati, M. Rebezov, K.R. Rengasamy, M.S. Mubarak, Superoxide dismutase: an updated review on its health benefits and industrial applications, Crit. Rev. Food Sci. Nutr. (2021) 1–19.
[99] M. Pantzar, Å. Ljungh, T. Wadström, Plasminogen binding and activation at the surface of Helicobacter pylori CCUG 17874, Infect. Immun. 66 (10) (1998) 4976–4980.
[100] M.A. Parry, X.C. Zhang, W. Bode, Molecular mechanisms of plasminogen activation: bacterial cofactors provide clues, Trends Biochem. Sci. 25 (2) (2000) 53–59.
[101] X.-Y. Meng, H.-X. Zhang, M. Mezei, M. Cui, Molecular docking: a powerful approach for structure-based drug discovery, Curr. Comput. Aided-Drug Des. 7 (2) (2012) 146–157.
[102] A.A. Ahmed, M.A. Rahman, M.A. Hossen, A.A. Reza, M.S. Islam, M.M. Rashid, M. K.J. Rafi, M.T.A. Siddiqui, A. Al-Noman, M.N. Uddin, Epiphytic Acampe ochracea orchid relieves paracetamol-induced hepatotoxicity by inhibiting oxidative stress and upregulating antioxidant genes in in vivo and virtual screening, Biomed. Pharmacother. 143 (2021), 112215.
[103] J. de Ruyck, G. Brysbaert, R. Blossey, M.F. Lensink, Molecular docking as a popular tool in drug design, an in silico travel, Adv. Appl. Bioinforma. Chem. 9 (1) (2016) 1–11.
[104] A.G. Atanasov, B. Waltenberger, E.M. Pferschy-Wenzig, T. Linder, C. Wawrosch, P. Uhrin, V. Temml, L. Wang, S. Schwaiger, E.H. Heiss, J.M. Rollinger, D. Schuster, J.M. Breuss, V. Bochkov, M.D. Mihovilovic, B. Kopp, R. Bauer, V. M. Dirsch, H. Stuppner, Discovery and Resupply of Pharmacologically Active Plant-derived Natural Products: A Review, Elsevier Inc, 2015, pp. 1582–1614.
[105] N.J.Fip Müller, COX-2 inhibitors, aspirin, and other potential anti-inflammatory treatments for psychiatric disorders, Front. Psychiatry 10 (2019) 375.
[106] R. Morphy, Z. Rankovic, The physicochemical challenges of designing multiple ligands, J. Med. Chem. 49 (16) (2006) 4961–4970.
[107] D.A. Filimonov, A.A. Lagunin, T.A. Gloriozova, A.V. Rudik, D.S. Druzhilovskii, P. V. Pogodin, V.V. Poroikov, Prediction of the biological activity spectra of organic compounds using the pass online web resource, Chem. Heterocycl. Compd. 50 (3) (2014) 444–457.
[108] D. Browne, B. McGuinness, J.V. Woodside, G.J. McKay, Vitamin E and Alzheimer's disease: what do we know so far? Clin. Inter. Aging 14 (2019) 1303–1317.
[109] S. Rizvi, S.T. Raza, F. Ahmed, A. Ahmad, S. Abbas, F. Mahdi, The role of vitamin e in human health and some diseases, Sultan Qaboos Univ. Med J. 14 (2) (2014) e157–e165.
[110] M. Adnan, M.N.U. Chy, A.T.M.M. Kamal, K.A.A. Chowdhury, M.A. Rahman, A.S. M. Ali Reza, M. Moniruzzaman, S.R. Rony, M.S. Nasrin, M.O.K. Azad, C.H. Park, Y.S. Lim, D.H. Cho, Intervention in neuropsychiatric disorders by suppressing inflammatory and oxidative stress signal and exploration of in silico studies for potential lead compounds from holigarna caustica (Dennst.) oken leaves, Biomolecules 10 (4) (2020).
[111] F. Cheng, W. Li, Y. Zhou, J. Shen, Z. Wu, G. Liu, P.W. Lee, Y. Tang, AdmetSAR: a comprehensive source and free tool for assessment of chemical ADMET properties, J. Chem. Inf. Model. 52 (11) (2012) 3099–3105.
[112] J. Lin, D. Sahakian, S. de Morais, J. Xu, R. Polzer, S. Winter, The role of absorption, distribution, metabolism, excretion and toxicity in drug discovery, Curr. Top. Med. Chem. 3 (10) (2005) 1125–1154.
[113] A.P. Li, Screening for human ADME/Tox drug properties in drug discovery, Drug Discov. Today (2001) 357–366.
[114] T. Hou, J. Wang, W. Zhang, X. Xu, ADME evaluation in drug discovery. 6. Can oral biavailability in humans be effectively predicted by simple molecular property-based rules? J. Chem. Inf. Model. 47 (2) (2007) 460–463.
[115] C.A. Lipinski, Lead- and drug-like compounds: the rule-of-five revolution, Drug Discov. Today. Technol. 1 (4) (2004) 337–341.
[116] D.F. Veber, S.R. Johnson, H.Y. Cheng, B.R. Smith, K.W. Ward, K.D. Kopple, Molecular properties that influence the oral bioavailability of drug candidates, J. Med. Chem. 45 (12) (2002) 2615–2623.
[117] J. Bicker, G. Alves, A. Fortuna, A. Falcão, Blood–brain barrier models and their relevance for a successful development of CNS drug delivery systems: a review, Eur. J. Pharm. Biopharm. 87 (3) (2014) 409–432.
[118] C. Lohmann, S. Hüwel, H.-J.J.Jodt Galla, Predicting blood-brain barrier permeability of drugs: evaluation of different in vitro assays, J. Drug Target. 10 (4) (2002) 263–276.
[119] F.X. Domínguez-Villa, N.A. Durán-Iturbide, J.G. Ávila-Zárraga, Synthesis, molecular docking, and in silico ADME/Tox profiling studies of new 1-aryl-5-(3-azidopropyl)indol-4-ones: potential inhibitors of SARS CoV-2 main protease, Bioorg. Chem. 106 (2021), 104497.